A DRUG DELIVERY APPROACH USING ZEOLITIC IMIDAZOLE FRAMEWORK-8 AND BIODEGRADABLE POLYMER COMPOSITE

by

Tahmid Faisal

APPROVED BY SUPERVISORY COMMITTEE:

_____

Dr. Jeremiah Gassensmith, Chair

_____

Dr. Ronald A. Smaldone, Co-Chair

_____

Dr. Mihaela C. Stefan

_____

Dr. Sheena D'Arcy

To all the people of my life who encouraged me on my way to knowledge and wisdom. Without their constant support I would have been grasping and suffocating in the labyrinth of ignorance and illiteracy.

A DRUG DELIVERY APPROACH USING ZEOLITIC IMIDAZOLE FRAMEWORK-8 AND BIODEGRADABLE POLYMER COMPOSITE

by

TAHMID FAISAL, M.PHARM.

THESIS

Presented to the Faculty of

The University of Texas at Dallas

in Partial Fulfillment

of the Requirements

for the Degree of

MASTER OF SCIENCE IN

CHEMISTRY

THE UNIVERSITY OF TEXAS AT DALLAS

August 2020

ACKNOWLEDGMENTS

First of all, I am grateful to Almighty God for my life. Then I would like to thank my thesis supervisors Dr. Jeremiah Gassensmith and Dr. Ronald Smaldone for their guidance and support throughout my graduate study at UT Dallas. It was a great opportunity to work under the supervision of two such nice people. The learning environment in their labs paved my way to understand chemistry. I can not help but show my gratitude to the members of the Gassensmith and Smaldone labs who were like my family. They helped me to understand the experiments and analyze the data. For the completion of my graduate study in the UT Dallas chemistry department, I am indebted to the professors who taught me the advanced chemistry subjects, showed me the path of excellence and guided me to think in the broader horizon. I am thankful to my parents and my wife for their constant encouragement and sacrifice for me. Lastly, without the support of The Department of Chemistry and Biochemistry, UT Dallas there would not be a thesis.

July 2020

A DRUG DELIVERY APPROACH USING ZEOLITIC IMIDAZOLE FRAMEWORK-8 AND BIODEGRADABLE POLYMER COMPOSITE

Tahmid Faisal, MS
The University of Texas at Dallas, 2020

Supervising Professors: Jeremiah Gassensmith, Chair
Ronald A. Smaldone, Co-Chair

Zeolitic imidazole frameworks (ZIF)-8 and polymers are potential platforms for drug delivery purpose. In this thesis these two drug delivery platforms have been combined to develop two types of drug delivery tools. To develop the first tool, model drug Cy5 dye and smURF protein have been loaded in ZIF-8 by biomineralization reaction and further encapsulated in biodegradable 50:50 ratio of poly (lactic-co-glycolic acid) polymer (PLGA) by solvent evaporation technique. This ZIF-8-PLGA polymer composite can be a promising tool to deliver a drug into the body over the course of long time slowly releasing it intact and protecting it from the environmental stressors. The second tool is the polymeric microneedles developed by using Fused Deposition Modelling based 3D printing. Poly Lactic acid was used to prepare microneedles patches. Model drug FITC Azide was loaded in ZIF-8 and further microneedles patches were loaded with those FITC containing ZIF-8 by biomineralization reaction at room temperature. Both drug delivery tools can be a robust platform to deliver drug and protein molecules by giving them protection from environmental stresses.

TABLE OF CONTENTS

LIST OF FIGURES

LIST OF TABLES

CHAPTER 1

INTRODUCTION

The world is fighting with different diseases. The need for different medicines and their delivery systems are increasing. For treatment purposes different drug delivery systems have been developed targeting specific diseases, routes and mechanism of action. These delivery systems are sometimes very effective for one kind of drug while it might not be suitable for another type. That depends on different pharmacokinetic and pharmacodynamic properties of the drug molecules e.g. stability in a specific route, dosing, absorption, distribution, metabolism and excretion. There are also several drug delivery routes like oral, nasal, parenteral/ injection, buccal, inhaler and suppository. Due to the different chemical and physiological aspects drug delivery methods vary for every drugs. Hence, suitable delivery method of drugs is an active area of research and development. In this thesis, two different drug delivery methods have been developed by combining metal organic framework and polymer.

1.1 Metal Organic Frameworks in Drug Delivery

Research in drug delivery is very challenging from a lack of availability of nanocarriers with minimal or no toxicity. An efficient nanocarrier for drug delivery should have several properties: (1) Drug entrapping with high loading, (2) controlled drug release avoiding burst effect, (3) engineerable surface and matrix degradation, (4) detectable release by analytical techniques, and (5) good biocompatibility and low toxicity. Currently, liposomes, functional hydrogels, micelles, nano-emulsions, nano particles like carbon nanotubes and gold or iron nanoparticles are being used as common drug delivery vehicles.[1-7]

These delivery methods can be categorized into inorganic and organic systems. Although organic systems can show biocompatibility, a controlled release mechanism can't be achieved all the time. On the other hand, inorganic systems like mesoporous silicon and silica can deliver adsorbed drugs in a more controlled manner but have very low loading capacity. So better methods are needed to address the aforementioned current limitations. Metal organic frameworks (MOFs), a mesoporous material group can be a robust tool for drug delivery.

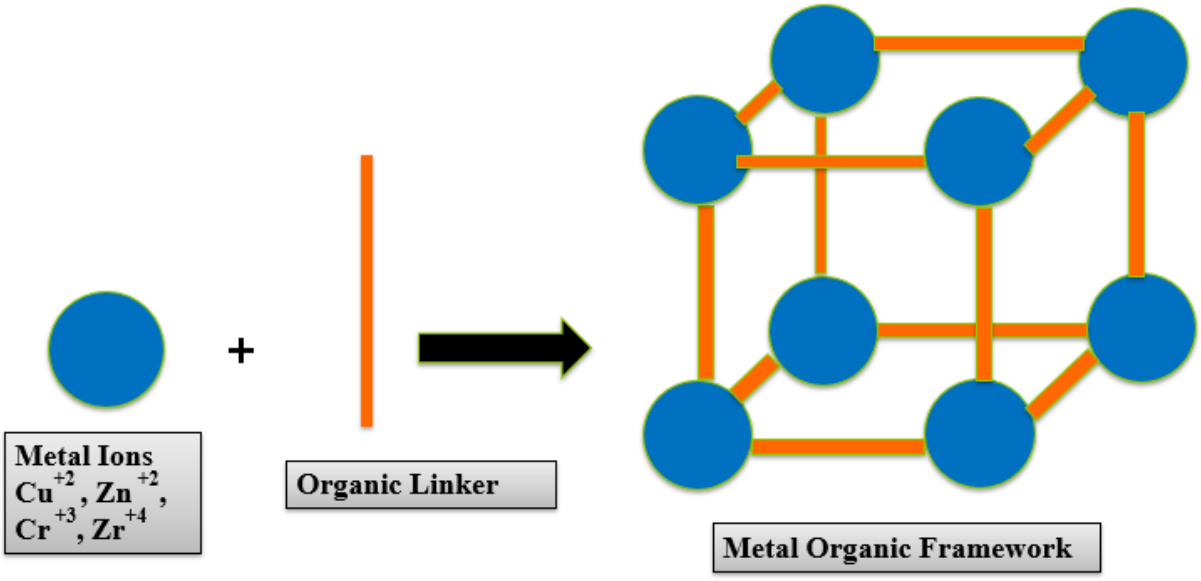

Figure 1.1: Metal organic framework (MOF) originated from metal ions and organic linker showing porous 3D structure.

Metal organic frameworks (MOFs) are highly porous crystalline materials made of metal-ion clusters linked by organic ligand struts in which zinc, copper, chromium, aluminum, zirconium, and other elements are commonly used to form frameworks with bivalent or trivalent aromatic carboxylic acids or N-containing aromatics.[8-10] Thousands of MOFs have been categorized in the Cambridge Structural Database (CSD) to date. [11-14] As MOFs have high metal content, high surface

area, tunable functionality, and high number of uniform pores they can be used in different purposes like catalysis,[15] gas separation,[16] gas storage,[17] luminescence[18] etc. Some are excellent nanocarrier of imaging agents,[19] nucleic acids,[20] and RNA-CRISPR complexes.[21]

1.1.1 MOF-5

As there are thousands of MOF structures, their stability in living systems should be considered if we want to use them for drug delivery purposes. IRMOF-1 or MOF-5 is a zinc based, widely studied MOF, which is unstable in humid environments. It has been found by molecular dynamic simulations that the framework of IRMOF-1 collapses at water content of 3.9% and higher due to the replacement of it's oxygen atom in the zinc coordination shell by the oxygen atom of water. [22-24] MOF Ni-CPO-27 showed only small amount (less than 10%) of dissolution after leaving in Bovine serum albumin for 4 days.[25]

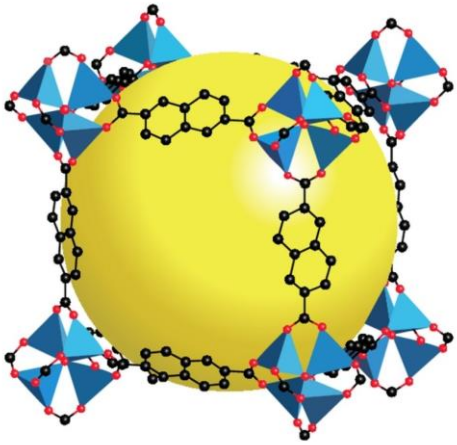

Figure 1.2 : MOF-5. Reprinted with permission from Ref 89. Copyright © 2003, Nature.

1.1.2 MIL MOFs The first family of MOF discovered as a potential drug delivery system is the Materials of Institute Lavoisier (MIL) family invented by Ferey and colleagues.[26] This MIL family arises from carboxylic acid bridging ligand and trivalent metal center. They have shown large pore

sizes of 25-34 Å and outstanding surface area of 3100-5900 m^2/g, which made them potential drug carrier. This pore size in mesoporous range is crucial for drug loading as microporous structures limit the drug loading capacity.[27] So far, different iron (III) based MILs delivered different drugs which is shown in the Table 1.1.

Table 1.1 : Particle Size, drug loading (wt%) in several porous iron (III) carboxylate nanoparticles. Reprinted with permission from Ref 28. Copyright © 2010, Nature Materials.

		MIL-89	MIL-88A	MIL-100	MIL-101 _NH_2	MIL-53
Organic linker		Muconic acid 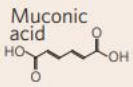	Fumaric acid 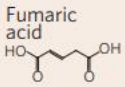	Trimesic acid 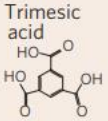	Amino terephthalic acid 	Terephthalic acid 
Crystalline structure						
Flexibility		Yes	Yes	No	No	Yes
Pore size (Å)		11	6	25 (5.6) 29 (8.6)	29 (12) 34 (16)	8.6
Particle size (nm)		50–100	150*	200	120	350*
Bu loading (efficiency) (%) 	13.4 × 3.5 amphiphilic	9.8 (4.2)	8.0 (3.3)	25.5 (31.9)	-	14.3 (17.9)
AZT-TP loading (efficiency) (%) 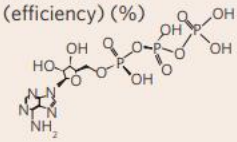	11.9 × 9.1 hydrophilic	-	0.60 (6.4)	21.2 (85.5)	42.0 (90.4)	0.24 (2.8)

Horcajada *et al.* also encapsulated ibuprofen in MIL-100 and MIL-101. MIL-100 contains pore size of 25-29 Å with pentagonal window openings of 4.8 Å and hexagonal windows of 8.6 Å. MIL-101, on the other hand, contains 29-34 Å pore size with a large window opening of 12Å for the pentagonal and 16Å for the hexagonal windows. The authors found that MIL-100 could uptake 0.35 g of ibuprofen/g of dehydrated MIL-100 and MIL-101 could uptake 1.4 g of ibuprofen/g dehydrated MIL-101 without significant change in their crystallinity.[28] This ibuprofen encapsulation variation can be attributed due to their pore sizes. This MIL-101 showed ibuprofen

release into the simulated body fluid up to 6 days. The π-π interaction between ibuprofen and aromatic ring was attributed to the elongated delivery time. On the other hand, MIL-53 showed breathing effect due to its capability of expansion of pores after heating. Upon heating 20 wt% loading was achieved and it took 3 weeks for complete delivery of ibuprofen in compared to MIL 101 and inorganic drug delivery MOF MCM-41 and amino MCM-41. A comparative study has been shown in Figure 1.3.

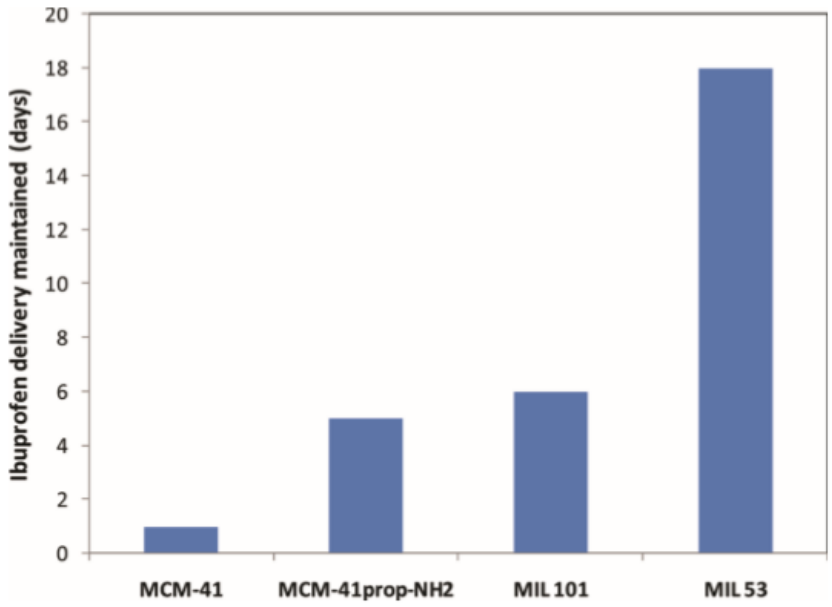

Figure 1.3 : Comparison of ibuprofen delivery from MCM-41, MCM41Prop-NH_2, MIL-101, and MIL-53. Reprinted with permission from Ref 28. Copyright © 2010, Nature Materials.

1.1.3 NU-1000 and NU-901 MOF

MOF NU-1000 is a mesoporous Zr based MOF synthesized from a node $Zr_6(\mu_3\text{-}O)_4(\mu_3\text{-}OH)_4(H_2O)_4(OH)_4$ and 1,3,6,8-(*p*-benzoate)pyrene (H_4TBAPy) linker. This MOF has shown outstanding stability and large pore size.[29-30] The terminal hydroxyl group allows post synthetic functionalization. Therefore NU-1000 has prospect in the biomedicine field.

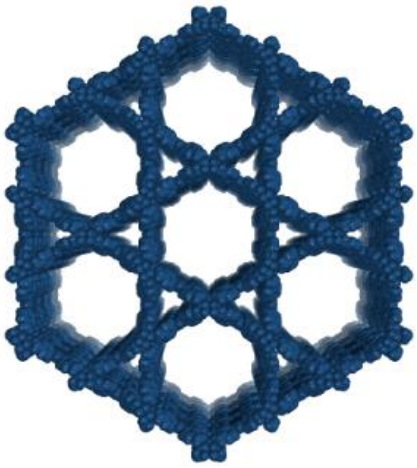

Figure 1.4 : NU-1000 showing mesoporous structure (https://3dprint.nih.gov/)

Xueyan *et al.* showed that large pore size of NU-1000 is conducive for efficient anticancer drug Doxorubicin loading (35 wt%) and the instability in PBS helps the controlled drug release.[31] They found that this system could release 65% DOX over 2 weeks period. They also PEGylated the DOX loaded NU-1000 crystals and found highest antitumor activity compared to free DOX and NU-1000. The cell viability study also showed that DOX and PEGylated DOX-NU 1000 composite showed cytotoxicity on the Hela Cell line with concentration from 0.1 to 10 µg/ml. In another research Shunzhi *et al.* showed NU-1000 and MOF-545 can be a good carrier of insulin protein by conjugating the MOFs surfaces with oligonucleotides. These MOFs acted as protein hosts, and their oligonucleotide-rich surfaces made them colloidally stable and ensured facile cellular entry. They achieved high loading and a 10-fold increment of cellular uptake compared to that of the native insulin. Insulin loaded MOF NU-1000 and MOF-545 showed 20% drug release over 96 hr period in DMEM buffer + 10 % blood serum (pH 7.0, 37ºC).[32]

1.1.4 Zeolitic Imidazole Framework (ZIF)

In 2006, a class of metal organic framework was found having unique bond angle of 145 between the metal and the imidazolate linker (M-Im-M angle), which mimics the Si-O-Si angle of zeolites-giving ZIFs zeolites like topology. They are made of tetrahedrally coordinated metal ions like zinc, cobalt, chromium, copper etc. linked by imidazole linker giving a sodalite like topology with an approximate BET surface area of 1600 m^2 /g and 6 ring pore aperture of 3.4 Å.[33] More than 100 ZIF MOFs have been discovered so far and being used for chemical and biomedical applications.

1.1.4.1 Zeolitic Imidazole Framework-8 (ZIF-8)

To date, ZIF-8 is a robust framework having high porosity that has been successfully used in different applications including drug delivery. In this thesis work, ZIF-8 has been selected as a candidate MOF material for it's exceptional chemical and thermal stability[34-35] and low cytotoxicity.[36] ZIF-8 can be synthesized with different methods: solvothermal, microwave assisted, sonochemical, mechanochemical, dry gel conversion, and microfluidic methods.[37] Among them, solvothermal one pot synthesis is preferentially used leading to biomineralization process to encapsulate drug molecules inside ZIF-8.[38] Chandan *et al.* showed ZIF-7 and ZIF-8 can be used as nanocarriers to encapsulate anticancer drug Doxorubicin. They observed that ZIF-7 remains intact in acidic condition while ZIF-8 releases drugs in controlled manner. The drug release from both ZIFs is also influenced by the presence of biomolecules like liposome. ZIF-8 has also been used in cancer chemotherapy by solving multidrug resistance.[39] Qing-Shan *et al.* introduced a novel drug delivery platform where ZIF-8 nano thick film was synthesized on the anticancer drug loaded mesoporous carboxylated silica nanoparticles and siRNA was electrostatically loaded in those ZIF-8 for efficient delivery. This delivery tool could preserve the

siRNA from the nuclease degradation and enabled it to downregulate multi drug resistance gene Bcl2 expression. At the same time the positive charge of ZIF-8 helped the silica nanoparticles to cross the cell membrane and enter into the cells.

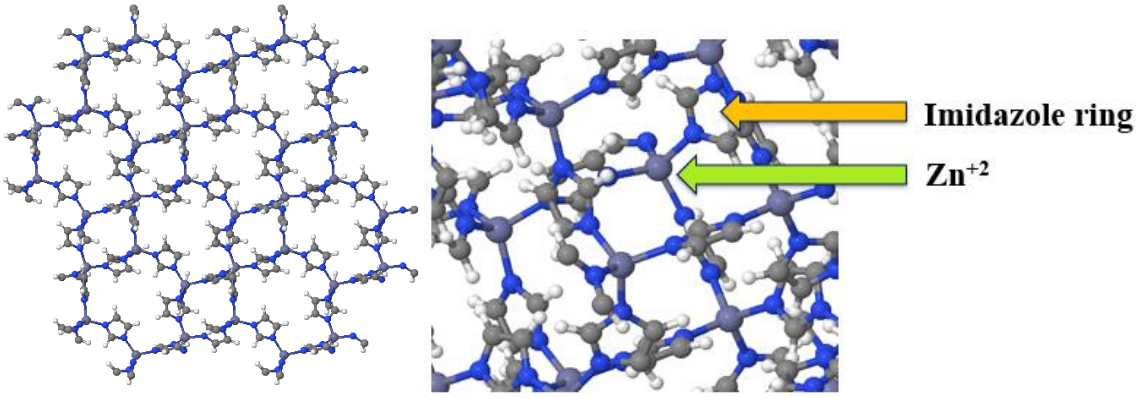

Figure 1.5 : Zeolitic Imidazole Framework-8 (Zinc is tetrahedrally linked to Imidazole linkers)

The unique stable crystal structure of ZIF-8 has an extraordinary capability to preserve drug and biomolecules inside it and prevent their degradation from chemical and environmental stressors. Luzuriaga *et al.* showed that after biomimetic encapsulation of vaccine candidate Tobacco Mosaic Virus (TMV) inside ZIF-8 layer, ZIF-8 showed protection of TMV from denaturing conditions by keeping all the viral activities intact.[35]

1.2 Polymeric Drug Delivery

Polymers are the most versatile class of materials that have changed our life in many aspects- from preparation of daily materials to the biomedical applications. Conventional drug delivery systems often are challenged by the successful delivery of desired dose to the target site. Most drugs taken by oral and parenteral injections are readily absorbed by the gastrointestinal tract and circulate to

the blood. Sometimes these molecules may be easily degraded by blood enzymes and the plasma drug concentration may not be at therapeutic level for a long time. In this case, polymers have made it easy for us to design controlled release of drug from their matrix by saving them from the cellular environmental factors like pH, temperature and enzymes. The chemical composition, molecular weight and stereoisomeric forms affects the rate of polymer degradation following release of drug molecule.[40] These biodegradable polymers may be found in natural and synthetic categories and can be useful in hydrophilic or hydrophobic drug molecules and proteins. A list of different polymers and delivered drug is listed in the Table 1.2.

Table 1.2 : Natural and synthetic polymers used in drug and protein delivery

Polymer	**Drug/Protein Delivered**
Natural	
Albumin	insulin, urokinase, YIGSR , gpl20 peptide, IIF-2, growth hormone[41-46]
Cellulose derivatives: Carboxymethyl cellulose	Acyclovir[47]
Collagen	Ibuprofen[48]
Fibrin	Doxorubicin[49]
Gelatin	Dopamine[50]
Hyaluronic acid	Insulin[51]

Table 1.2, continued

Synthetic	
Polyesters	
Poly lactic acid (PLA)	Vaccine[52], HSA[53], insulin[54], LHRH[55]
Poly (lactic-co-glycolic acid) (PLGA)	Carbonic anhydrase[56], IL-2[57], G-CSF[58], insulin[59], LHRH[60-63], Paclitaxel[64]
Poly (ß-hydroxybutyrate)	Tissue engineering scaffolds[65-67]
Poly (caprolactone)	Rhodamine B, Ibuprofen, Camptothecin[68]
Poly (dioxanone)	Radiosensitizer (VE822) in brain tumor[69]
Polyanhydrides	
Poly (sebacic acid)	Paclitaxel[70]
Poly (adipic acid)	Chlorambucil, Glutamine[71]
Poly (terephthalic acid)	Bone regeneration therapy[72]
Polyamides	
Poly(imino carbonates), poly amino acids	Poly(imino carbonates), poly amino acids
Others	
Poly ((hydroxypropyl) methacrylamide)	Doxorubicin[74]
Poly (vinyl alcohol)	5-Fluorouracil[75]
Poly (vinylpyrrolidone)	Chymotrypsin[76], BSA[77]
Maleic anhydride—alkyl vinyl ether copolymers	IFN alpha , HSA[78]

Table 1.2, continued

Pluronic polyols	Doxorubicin, Leishmeniasis therapy[79]
Poly(acrylic acid)	Chlorine dioxide[80], Iron oxide[81]
Poly(cyanoacrylates)	Ocular drug delivery[82]
Poly(anhydrides)	Docetaxel[83]
Polyurethanes, poly-ortho esters, poly dihydropyrans, polyacetals	Cancer Gene therapy[84], 5-FU[85]
Cellulose derivatives: Ethyl cellulose, cellulose acetate, cellulose acetate propionate	Catechin[86], 5-Amino salicylic acid[87]
Silicones: Polydimethylsiloxane, colloidal silica	Lovastatin[88]

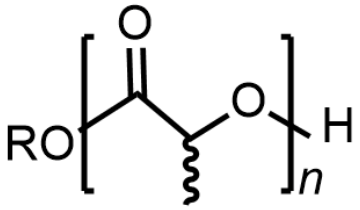

Poly (lactide) (PLA)

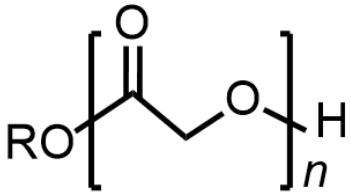

Poly (glycolide) (PGA)

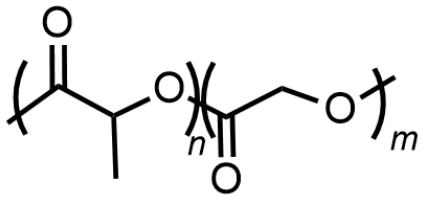

Poly (lactide-co-glycolide) (PLGA)

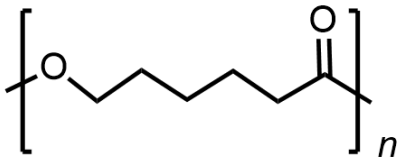

Poly (caprolactone) (PCL)

Figure 1.6 : Some polymers used in drug delivery application

The polymers may degrade by different mechanisms and release of drugs would also be influenced by that. In most cases, nonbiodegradable polymer matrix releases drug in diffusion-controlled manner and drugs with low permeability can be released through the channels and pores created by the dissolved drug phase.[7] Biodegradable polymers may undergo degradation or erosion. Degradation is a chemical process, whereas erosion is a physical phenomenon dependent on diffusion dissolution and process. Erosion can occur by either surface or bulk erosion- depending on the chemical structure of the polymer backbone. Surface erosion represents the situation when the rate of erosion exceeds the rate of water permeation into the polymer bulk. This erosion kinetics and rate of drug release (zero order) are highly reproducible. Bulk erosion occurs when water permeation into the bulk of the matrix happens at a faster rate than erosion. Most biodegradable polymers for drug delivery show bulk erosion. The use of nanoparticle or microparticle formulations possessing massive surface areas results in bulk- and surface-eroding materials that show similar erosion kinetics. Further, the erosion process can be manipulated by modifying the surface area of the DDS or by including hydrophobic monomer units in the polymer.[90]

1.2.1 Poly Lactic co Glycolic acid (PLGA) based Drug Delivery

Poly lactic co glycolic acid (PLGA) is a promising biodegradable and biocompatible co block polymer, which is an ester of different molar ratio of poly lactic acid (PLA) and poly glycolic acid (PGA) monomers. The ratio of these two monomers can change the overall degradation profile of the polymer. When PLA is copolymerized with crystalline PGA, it reduces the degree of crystallinity of PLGA and as a result increase the rate of hydration and hydrolysis. As a rule, higher content of PGA leads to quicker rates of degradation with an exception of 50:50 ratio of PLA/PGA, which exhibits the fastest degradation.[91]

1.3 3D Printing Technology

Three- dimensional printing or 3D printing is a technology to build up objects from computer aided design (CAD) models.[92] This technique is also attributed to the process of joining materials (melted solid or liquid or powders) layer by layer. Hence this is also known as 'Additive manufacturing'. The concept of additive manufacturing first came from Hideo Kodama of Japan in 1981 who invented additive manufacturing method of thermoset polymer to make plastic models by UV exposure. The first patent for computer aided manufacturing process came in 1984 by Bill Masters, an American entrepreneur. In the same year Chuck Hull invented 'Stereolithography'- a process to build 3D objects by curing photopolymers with UV laser light. The mostly used 3D printing machine widely used so far is the Fused Deposition Model printer for printing plastic materials, was invented in 1988 by S. Scott Crump and commercialized in 1992 by his company Stratasys. Although metal sintering and melting emerged in 1980 and 1990 respectively, the actual additive manufacturing for metals and solid powders by computer aided setup was developed later.

Extrusion Based 3D Printing

Extrusion based 3D printing is a method to fabricate 3D materials by depositing on a surface by predetermined computer aided models and printing parameters. This method can be categorized into three techniques.

(a) Fused Deposition modelling- which is a process to make objects by thermoplastic polymers. [93] In this process thermoplastic polymer filament is feed into a heated nozzle in 3D printer at a specific temperature and deposit on a heated bed. The thermoplastic polymers get cured at room temperature by turning into the 3D models.

(b) Direct ink writing- it's a process to tune rheological properties of polymers, gels, metals and ceramics and get them deposited by robotic controlled nozzle to generate 3D scaffolds. [94] This method has the advantage of incorporation of high mechanical and desired chemical properties to the objects.

(c) Bioprinting- is an advanced 3D printing method to fabricate structures by crosslinking hydrogels or living tissues, that can be further processed with the cell growth factors.[95] This method is very popular and useful in incorporating chemical characteristics in hydrogels and biomedical engineering in tissue damage cases.

Vat or Photopolymerization based 3D Printing

This printing method uses photopolymer resins in a vat and construct objects by shining UV light on the polymer bed and fabricate material layer by layer or point by point.[96] This is done by photopolymerization reactions by UV light. When the UV light from a source is focused on the resin bed, the polymer gets hardened or cure and turns into the predetermined shapes and models. This is the finest method of 3D printing that offers high resolution. Depending on the fabrication mechanism, there are three types of photopolymerization 3D printing methods.

(a) Stereolithography (SLA)- this method creates object by curing acrylate, methacrylate, epoxy or vinyl ether like photopolymer resins by UV laser in a point by point structure. [97] This is done by chain growth polymerization mechanism. Printing resolution is 10 µm.

(b) Digital Light Processing (DLP)- this method is capable of using LED light source from UV to visible range which cure each layer at once.[98] Cured layers are not in direct contact with air. Objects have resolution of 10-50 µm.

(c) Continuous Liquid Interface Production (CLIP)- continuous fabrication of model from a dead zone is done by inhibiting free radical polymerization by using a oxygen permeable window in the 3D printer.[99] This method offers the fastest and highest resolution printing.

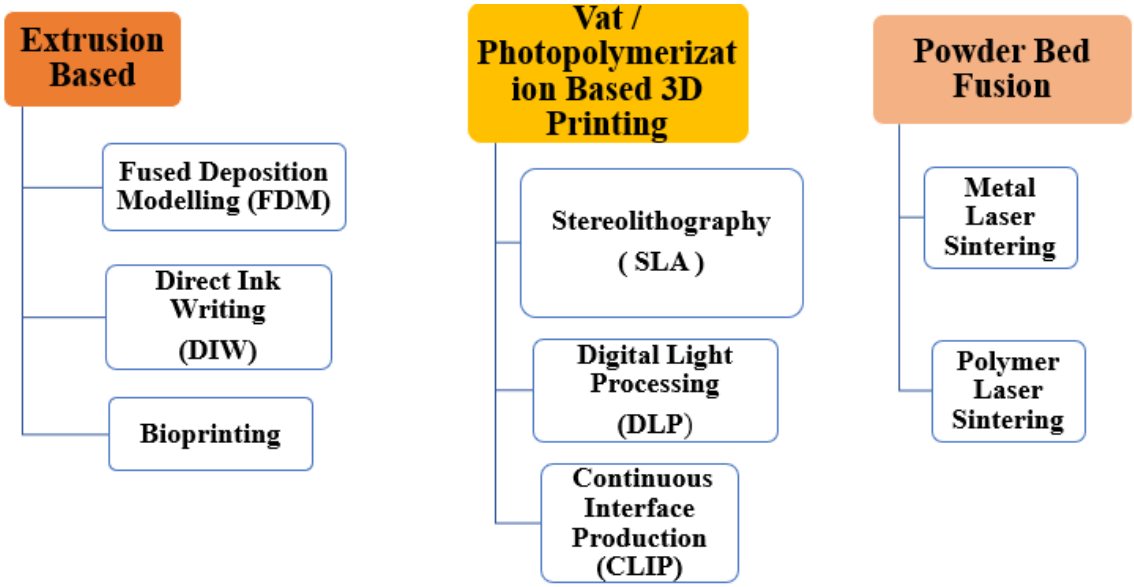

Figure 1.7 : Different 3D printing technology based on extrusion, photopolymerization and powder bed fusion

Powder Bed Fusion

This method is for fabricating metal or powdered materials by sintering at a high temperature. This is also good for fusion of two different types of materials.

1.3.1 Fused Deposition Modelling (DFM) Based 3D Printing

This printing method is also known as FFF or Fused Filament Fabrication where thermoplastic polymer filaments are inserted through a nozzle of FDM 3D printer. This nozzle can be heated and controlled by a robotic scaffold by commanding from a software. The polymer filaments get heated at their specified melting temperatures (Table 1.3) and gets deposited on the printing bed. At room temperature they get hardened and transformed into 3D objects.

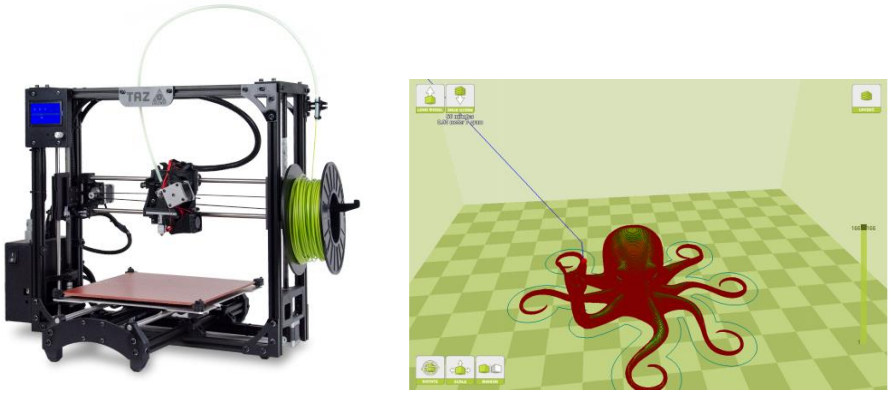

Figure 1.8 : FDM 3D Printer (left) and Cura LulzBot software control panel (right). Reprinted from LulzBot™ TAZ 5 User Manual. Copyright © 2015 Aleph Objects, Inc.

1.3.2 Microneedles based drug delivery

Microneedles are transdermal painless drug delivery tool that is alternative to painful needles.[101] These needles usually have height of 10-2000 μm and width of 10-90 μm. Microneedles can create pore into the skin and transfer drug to the transdermal layer directly. There are four types of

Table 1.3 : Recommended printing temperatures for different polymer filaments. Reprinted from LulzBot™ TAZ 5 User Manual. Copyright © 2015 Aleph Objects, Inc.

Filament type	Nozzle temp (ºC)	Bed temp (ºC)	Removal temp (ºC)
PLA	195-215	60	45
ABS	230-250	110	50
Polycarbonate	260-300	110	50
HIPS	230-250	110	50
Stainless Steel PLA	220-230	60	50
Conductive PLA	215-230	60	50
Polycaprolactone	70-140	45	30

microneedles, each type has different way of transferring drug molecules to the skin- (1) solid microneedles, (2) coated microneedles, (3) dissolving microneedles and (4) hollow microneedles. Each type has unique purpose depending on the nature of drug or protein molecules to be delivered and the desired rate of delivery.

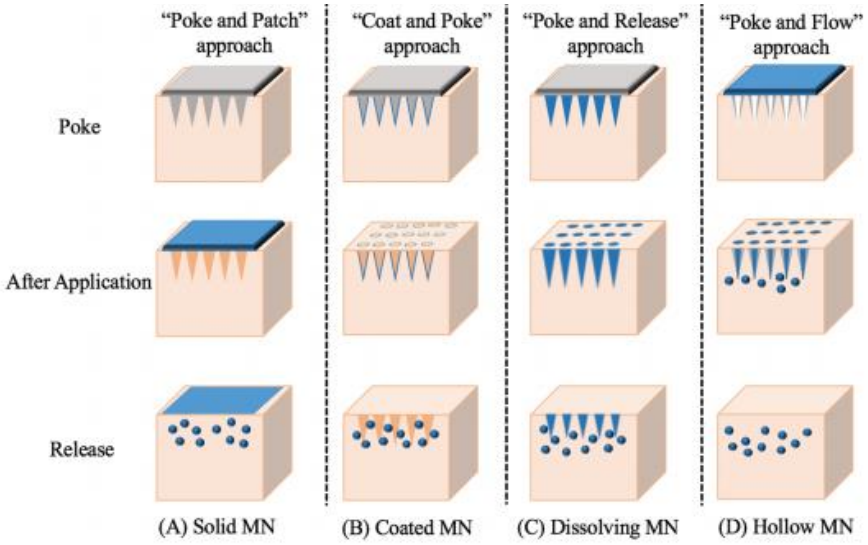

Figure 1.9 : Different types of Microneedles patches. Reprinted with the permission of Ref 100. Copyright © 2017 American Scientific Publishers.

In this thesis work, polymeric microneedles patches were made with poly lactic acid thermoplastic polymer by FDM 3D printing method. The patches were further coated with FITC loaded ZIF-8 by biomineralization reaction.

1.4 References

1. Peer, D.; Karp, J.M.; Hong, S.; Farok, O.C.; Margalit, R.; Langer, R. Nanocarriers as an Emerging Platform for Cancer Therapy. *Nat. Nanotechnol*. **2007**, *2*, 751.

2. Gref, R.; Amiel, C.; Molinard, K.; Daoud-Mahammed, S.; Sebille, B.; Gillet, B.; Beloeil, J. C.; Ringard, C.; Rosilio, V.; Poupaert, J.; Couvreur, P. New Self-Assembled Nanogels Based on Host-Guest Interactions: Characterization and Drug Loading. *J. Controlled Release*. **2006**, *111*, 316.

3. Gref, R.; Minamitake, Y.; Peracchia, M. T.; Trubetskoy, V.; Torchilin, V.; Langer, R. Biodegradable Long-Circulating Polymeric Nanospheres. *Science*. **1994**, *263*, 1600.

4. Gabizon, A.A.; Stealth Liposomes and Tumor Targeting: One Step Further in the Quest for the Magic Bullet. *Clin. Cancer Res.* **2001**, *7*, 223.

5. Hasan, A.S.; Socha, M.; Lamprecht, A.; El Ghazouani, F.; Sapin, A.; Hoffman, A.; Maincent, P.; Ubrich, N.; Effect of the Microencapsulation of Nanoparticles on the Reduction of Burst Release. *Int. J. Pharm*. **2007**, *344*, 53.

6. Kizilel, S.; Perez-Luna, V. H.; Teymour, F. Photopolymerization of Poly (Ethylene Glycol) Diacrylate on Eosin-Functionalized Surfaces. *Langmuir*. **2004**, *20*, 8652.

7. Kizilel, S.; Sawardecker, E.; Perez-Luna, V. H.; Teymour, F. Sequential Formation of Covalently Bonded Hydrogel Multilayers through Surface Initiated Photopolymerization. *Biomaterials*. **2006**, *27*, 1209.

8. Hayashi, H; Cote, A. P.; Furukawa, H.; O'Keefee, M; Yaghi, O. M. Zeolite A imidazole frameworks. *Nat. Mater*. **2007**, *6*, 501-506.

9. S., Tanaka**;** R., Miyashita; Aqueous-System-Enabled Spray-Drying Technique for the Synthesis of Hollow Polycrystalline ZIF-8 MOF Particles; *ACS Omega***. 2017,** *2*, 10, 6437-6445.

10. P.i Cui; P. Wang;Yue Zhao; W. Sun; Fabrication of Desired Metal–Organic Frameworks via Postsynthetic Exchange and Sequential Linker Installation; *Crystal Growth & Design.* **2019**, *19*, 2, 1454-1470.

11. Schlichte, K.; Kratzke,T.; Kaskel, S. Improved Synthesis, Thermal Stability and Catalytic Properties of the Metal Organic Framework Compound $Cu_3(Btc)_2$. *Microporous Mesoporous Mater.* **2004**, *73*, 81.

12. Pichon, A.; Lazuen-Garay, A.; James, S. L. Solvent-Free Synthesis of a Microporous Metal Organic Framework. *Cryst. Eng. Comm.* **2006**, *8*, 211.

13. Rood, J.A.; Noll, B.C.; Henderson, K.W. Synthesis, Structural Characterization, Gas Sorption and Guest-Exchange Studies of the Lightweight Porous Metal-Organic Framework Alpha--[Mg3(O2CH)6]. *Inorg. Chem*. **2006**, *45*, 5521.

14. Yaghi, O. M.; Li, H. L. Hydrothermal Synthesis of a Metal Organic Framework Containing Large Rectangular Channels. *J. Am. Chem. Soc*. **1995**, *117*, 10401.

15. Zhu, L.; Liu, X.; Jiang, H.; Sun. L.Metal-Organic Frameworks for Heterogeneous Basic Catalysis. *Chem. Rev*. **2017**, *117*, 8129.

16. Li, J.; Sculley, J.; Zhou. H. Metal-Organic Frameworks for Separations. *Chem. Rev*. **2012**, *112*, 869.

17. Babarao, R.; Jiang, J. Molecular Screening of Metal Organic Frameworks for CO2 Storage. *Langmuir*. **2008**, *24*, 6270.

18. Jin, Z.; Zhu, G. S.; Zou, Y. C.; Fang, Q. R.; Xue, M.; Li, Z. Y.; Qiu, S. L. Synthesis, Structure and Luminescent Property of a New 3D Porous Metal-Organic Framework with Rutile Topology. *J. Mol. Struct*. **2008**, *871*, 80.

19. Xu, R.; Wang, Y.; Duan, X.; Lu, K.; Micheroni, D.; Hu, A.; Lin, W. Nanoscale Metal Organic Frameworks for Ratiometric Oxygen Sensing in Live Cells. *J. Am. Chem. Soc.* **2016**, *138*, 2158.

20. He, C.; Lu, K.; Liu, D.; Lin, W. Nanoscale Metal-Organic Frameworks for the Co Delivery of Cisplatin and Pooled siRNAs to Enhance Therapeutic Efficacy in Drug Resistant Ovarian Cancer Cells. *J. Am. Chem. Soc*. **2014**, *136*, 5181.

21. Alsaiari,S. K.; Patil, S.; Alyami, M; Alamoudi,K O.; Aleisa, F. A. ; Merzaban,J. S.; Li, Mo; Khashab, N. M. Endosomal Escape and Delivery of CRISPR/Cas9 Genome Editing Machinery Enabled by Nanoscale Zeolitic Imidazolate Framework. *J. Am. Chem. Soc.* **2018**, *140*, 1, 143-146.

22. Greathouse, J. A.; Allendorf, M. D. The Interaction of Water with MOF-5 Simulated by Molecular Dynamics. *J. Am. Chem. Soc*. **2006**, *128*, 10678.

23. Bahr, D.F.; Reid, J.A.; Mook, W. M.; Bauer, C.A.; Stumpf, R.; Skulan, A. J.; Moody, N. R.; Simmons, B. A.; Shindel, M. M.; Allendorf, M. D. Mechanical Properties of Cubic Zinc Carboxylate IRMOF-1 Metal-Organic Framework Crystals. *Phys. Rev. B*. **2007**, *76*, 184106.

24. Kaye, S. S.; Dailly, A.; Yaghi, O. M.; Long, J. R. Impact of Preparation and Handling on the Hydrogen Storage Properties of Zn4O (1,4-Benzenedicarboxylate)3 (MOF-5). *J. Am. Chem. Soc*. **2007**, *129*, 14176.

25. Hinks, N. J.; McKinlay, A.C.; Xiao, B.; Wheatley, P. S.; Morris, R. E. Metal Organic Frameworks as NO Delivery Materials for Biological Applications. *Microporous Mesoporous Mater.* **2010**, *129*, 330.

26. Ferey, G.; Mello, C.; Serre, C.; Millange, F.; Dutour, J.; Surble, S.; Margiolaki, I. A Chromium Terepthalate-Based Solid with Unusually Large Pore Volumes and Surface Area. *Science*. **2005**, *309*, 2040.

27. Horcajada, P.; Serre, C.; Vallet-Regi, M.; Sebban, M.; Taulelle, F.; Ferey,G. Metal-Organic Frameworks as Efficient Materials for Drug Delivery. *Angew. Chem., Int. Ed.* **2006**, *45*, 5974.

28. Horcajada, P.; Chalati, T.; Serre, C.; Gillet, B.; Sebrie, C.; Baati, T.; Eubank, J.F.; Heurtaux, D.; Clayette, P.; Kreuz, C.; Chang, J.S.; Hwang, Y. K.; Marsaud, V.; Bories, P. N.; Cynober, L.; Gil, S.; Ferey, G.; Couvreur, P.; Gref, R. Porous Metal-Organic-Framework Nanoscale Carriers as a Potential Platform for Drug Delivery and Imaging. *Nat. Mater*. **2010**, *9*, 172.

29. Mondloch, J. E.; Bury, W.; Fairen-Jimenez, D.; Kwon, S.; DeMarco, E. J.; Weston, M. H.; Sarjeant, A. A.; Nguyen, S. T.; Stair, P. C.; Snurr, R. Q.; Farha, O. K.; Hupp, J. T. Vapor-Phase Metalation by Atomic Layer Deposition in a Metal-Organic Framework. *J. Am. Chem. Soc.* **2013**, *135* (28), 10294- 10297.

30. Teplensky, M. H.; Fantham, M.; Li, P.; Wang, T. C.; Mehta, J. P.; Young, L. J.; Moghadam, P. Z.; Hupp, J. T.; Farha, O. K.; Kaminski, C. F.; Fairen-Jimenez, D. Temperature Treatment of Highly Porous Zirconium-Containing Metal-Organic Frameworks Extends Drug Delivery Release. *J. Am. Chem. Soc*. **2017**, *139 (22)*, 7522-7532.

31. Zhao, X.; Liu, H.; Hu, C.; Liu, Y ; Pang, M.; Lin. J .Controllable Synthesis of Monodispersed NU-1000 Drug Carrier for Chemotherapy. *ACS Appl. Bio Mater.* **2019**, *2*, 4436−444.

32. Wang, S. Z.; Chen, Y. J.; Wang, S. Y.; Li, P.; Mirkin, C. A.; Farha, O. K. DNA-Functionalized Metal-Organic Framework Nanoparticles for Intracellular Delivery of Proteins. *J. Am. Chem. Soc*. **2019**, *141 (6)*, 2215−2219.

33. Tsai, C.; Langner, E..H.G. The effect of synthesis temperature on the particle size of nano-ZIF-8. *Micro. Meso. Mater*. **2016**, *221*, 8-13.

34. Park,K.S; Ni, Z.;Côté, A.P.; Choi, J.Y.; Huang, R.; Uribe-Romo, F.J.; Chae, H.K.; O'Keeffe, M.;Yaghi, O. Exceptional chemical and thermal stability of zeolitic imidazolate frameworks. *Proc Natl Acad Sci U S A*. **2006**, *103*, 10186-10191.

35. Luzuriaga, M. A.; Welch, R.P.; Dharmarwardana, M.; Benjamin, C. E.; Li, S.; Shahrivarkevishahi, A.; Popal, S.; Tuong, L.H.; Creswell, C.T.; Gassensmith, J. J. Enhanced Stability and Controlled Delivery of MOF-Encapsulated Vaccines and Their Immunogenic Response In Vivo *ACS Appl. Mater. Interfaces*. **2019**, *11*, 10, 9740–9746.

36. Vasconcelos, I. B.; Silva, T. G.; Militão, G. C. G.; Soares, T. A.; Rodrigues, N. M.; Rodrigues, M.O.; Costa, N. B. ; Freire, R. O.; Junior, S. A. Cytotoxicity and slow release of the anti-cancer drug doxorubicin from ZIF-8. *RSC Adv*. **2012**, *2*, 9437-9442.

37. Lee, Y.; Jang, M. ; Cho, H.; Kwon, H; Kim, .; S. ; Ahn, W. ZIF-8: A comparison of synthesis methods. *Chem. Eng. J*. **2015**, *271*, 276-280.

38. Adhikari, C.; Das, A.; Chakraborty, A. Zeolitic Imidazole Framework (ZIF) Nanospheres for Easy Encapsulation and Controlled Release of an Anticancer Drug Doxorubicin under Different External Stimuli: A Way toward Smart Drug Delivery System. *Mol. Pharmaceutics*. **2015**, 12, 3158−3166.

39. Pan, Q ; Chen, T.; Nie, C.; Yi, J.; Liu, C.; Hu, Y.; Chu,X. In Situ Synthesis of Ultrathin ZIF-8 Film-Coated MSNs for Codelivering Bcl 2 siRNA and Doxorubicin to Enhance Chemotherapeutic Efficacy in Drug-Resistant Cancer Cells. *ACS Appl. Mater. Interfaces* **2018**, *10*, 33070−33077.

40. Kang, J.; Schewendeman, S.P. Pore Closing and Opening in Biodegradable Polymers and Their Effect on the Controlled Release of Proteins. *Mol. Pharmaceutics.* **2007**, *4*, 1, 104-118.

41. Goosen, M. F. A.; O'Shea, G. M.; Gherapetian, M.; Chow, S.; Sun, A. M. Optimization of microencapsulation parameters: semipermeable microcapsules as an artificial pancreas. *Biotechnol. Bioeng*. **1985**, *27*, 146-150

42. Bhargave, K.; Ando, Y. Immobilization of active urokinase on albumin microspheres: Use of a chemical dehydrant and process monitoring. *Pharm. Res.* **1992**, *9*, 776-781.

43. Kolodny, N.; Robey, F. A. Conjugation of synthetic peptides to proteins: quantitation from S-carboxymethylcysteine released upon acid hydrolysis. *Anal. Biochem*. **1990**, *187*, 136-140.

44. Zegers, N.; Gerritse, K.; Been, C.; Boersma, W.; Claassen, E. An improved conjugation method for controlled covalent coupling of synthetic peptides to proteins using glutaraldehyde in a dialysis method. *J. Immunol. Methods*. **1990**, *130*, 195-200.

45. Isoai, A.; Goto-Tsukamoto, H.; Murakami, K.; Akedo, H.; Kumagai, H. A potent anti-metastatic activity of tumor invasion-inhibiting factor-2 and albumin conjugate. *Biochem. Biophys. Res. Commun*. **1993**, *192*, 7-14.

46. Poznansky, M. J.; Halford, J.; Taylor, D. Growth hormone - albumin conjugates. Reduced renal toxicity and altered plasma clearance. *FEBS Lett*. **1988**, *239*, 18-22.

47. Malik, N.S; Ahmad, M; Minhas, M.U. Cross-linked β-cyclodextrin and carboxymethyl cellulose hydrogels for controlled drug delivery of acyclovir. *PLoS One*. **2017**,*12*.

48. Vulpe, R; Popa, M.; Picton L; Peptu, CA; Tudorachi, N; Verestiuc, L. Scaffolds Based on Collagen, Hyaluronan and Sericin with Potential Applications as Controlled Drug Delivery System. *J Nanosci Nanotechnol*. **2018** , *18*, 3, 1528-1533.

49. Viale, M; Monticone, M; Maric, I. Characterization of drug release from fibrin gels loaded with different pharmaceutical and experimental doxorubicin formulations. *Pharmacol Rep*. **2018**, *70*, 4, 760-765.

50. Ren Y, Zhao X, Liang X, Ma PX, Guo B. Injectable hydrogel based on quaternized chitosan, gelatin and dopamine as localized drug delivery system to treat Parkinson's disease. *Int. J. Biol. Macromol*. **2017**,*105*, 1,1079-1087.

51. Ren Y, Zhao X, Liang X, Ma PX, Guo B. Injectable hydrogel based on quaternized chitosan, gelatin and dopamine as localized drug delivery system to treat Parkinson's disease. *Int.J.Biol.Macromol*. **2017**;*105*,1,1079-1087.

52. Peres, C.; Matos, A.I.; Conniot, J.; Poly (lactic acid)-based particulate systems are promising tools for immune modulation. *Acta. Biomater*. **2017** , *48*, 41-57.

53. Verrecchia, T., Huve, P.; Bazile, D.; Veillard, M.; Spenlenhauer, G.; Couvreur, P. Adsorption/desorption of human serum albumin at the surface of polydactic acid) nanoparticles prepared by a solvent evaporation process, *J. Biomed. Mater. Res*. **1993**, *27*, 1019-1028.

54. Kwong, A. K.; Chou, S.,; Sun, A. M.; Sefton, V.; Goosen, M. F. A. In vitro and in vivo release of insulin from polydactic acid) microbeads and pellets. *J. Controlled Release.* **1986**, *4*, 47-62.

55. Okada, H.; Doken, Y.; Ogawa, Y.; Toguchi, H. Preparation of three-month depot injectable microspheres of leuprorelin acetate using biodegradable polymers. *Pharm. Res.* **1994**, *11*, 1143-1147.

56. Lu, W.; Park, T. G.; Protein release from poly- (lactic-co-glycolic acid) microspheres: Protein stability problems. *PDA J. Pharm. Sci. Technol*. **1995**, *49*, 13-19.

57. Hora, M. S.; Rana, R. K.; Nunberg, J. H.; Tice, T. H.; Gilley, R. M.; Hudson, E. Controlled release of interleukin-2 from biodegradable microspheres. *Bio. Technology*. **1990**, *8*, 755-758.

58. Cambie, R.; Timms, D.; Wilkins on, A. J. Continuous release pharmaceutical compositions. *U.S. Patent*. **1994**, 5,320,840.

59. Chang, T. M. S. Biodegradable semipermeable microcapsules containing enzymes, hormones and vaccines, and other biologicals. *J. Bioeng*. **1976**, *1*, 25.

60. Hutchinson, F. G.; Furr, B. J. A. Biodegradable polymers for the sustained release of peptides. *Biochem. Soc. Trans*. **1985**, *13*, 520-523.

61. Ogawa, Y.; Okada, H.; Yamamoto, M.; Shimamoto, T. In vivo .profiles of leuprolide acetate from microcapsules prepared with polylactic acids or copolylactic/glycolic) acids and in vivo degradation of these polymers. *Chem. Pharm. Bull*. **1988**, *36*, 2576-2581.

62. Ogawa, Y.;Yamamoto, M; Okada, H.; Yashiki, T.; Shimamoto, T. A new technique to efficiently entrap leuprolide acetate into microcapsules of polylactic acid or copolydactic/glycolic) acid. *Chem. Pharm. Bull*. **1988**, *36*, 1095-1103.

63. Okada, H.; Inoue, Y.; Heya, T.; Ueno, H.; Ogawa, Y.; Toguchi, H. Pharmacokinetics of once-a-month injectable microspheres of leuprolide acetate. *Pharm. Res*. **1991**, *8*, 787- 791.

64. Chen, Y.; Yang, Z.; Liu, C. Synthesis, characterization, and evaluation of paclitaxel loaded in six-arm star-shaped poly (lactic-co-glycolic acid). *Int J Nanomedicine*. **2013**,*8*,4315-4326.

65. Dave, P.; Gross, R. A.; Brucato, C.; Wong, S.; McCarthy, S. P. Biodegradation of blends containing poly(3-hydroxybutyrate-co-valerate). *Biotechnology and Polymers*. **1991**, 53-61.

66. Amaro, L.; Correia, D.M.; Marques-Almeida, T.; Tailored Biodegradable and Electroactive Poly(Hydroxybutyrate-Co-Hydroxyvalerate) Based Morphologies for Tissue Engineering Applications. *Int J Mol Sci*. **2018**, *19*, 8, 2149.

67. Castellano, D.; Sanchis, A.; Blanes, M. Electrospun poly(hydroxybutyrate) scaffolds promote engraftment of human skin equivalents via macrophage M2 polarization and angiogenesis. *J. Tissue Eng. Regen Med*. **2018**, *12*, 2, 983-994.

68. Surnar, B.; Jayakannan, B. Stimuli-Responsive Poly(caprolactone) Vesicles for Dual Drug Delivery under the Gastrointestinal Tract. *Biomacromolecules*. **2013**, *14*, 12, 4377-4387.

69. Chen, E.M.; Quijano, A.R.; Seo, Y.E. Biodegradable PEG-poly (ω-pentadeca lactone-co-p-dioxanone) nanoparticles for enhanced and sustained drug delivery to treat brain tumors. *Biomaterials*. **2018**, *178*, 193-203.

70. Shikanov, A.; Ezra, A.; Domb, A.J. Poly (sebacic acid-co-ricinoleic acid) biodegradable carrier for paclitaxel effect of additives. *J. Control Release*. **2005**, *105*, 1-2, 52-67.

71. Tabasi, M.A; Amanlou, M.; Siadat, S.D. Novel molecular anti-colorectal cancer conjugate: chlorambucil-adipic acid dihydrizide-glutamine. *Anticancer Agents Med Chem*. **2013**, *13*, 9, 1449-1459.

72. Natarajan, J.; Madras, G.; Chatterjee, K. Poly(ester amide)s from Poly(ethylene terephthalate) Waste for Enhancing Bone Regeneration and Controlled Release. *ACS Appl Mater Interfaces*. **2017**, *9*, 34, 28281-28297.

73. Kohn, J.; Langer, R. Poly (iminocarbonates) as potential biomaterials. *Biomaterials*. **1986**, *7*, 3, 176-182.

74. Zhang, J.; Tang, H.; Shen, Y.; Yu, Q.; Gan, Z. Shell-Sheddable Poly (N-2-hydroxypropyl methacrylamide) Polymeric Micelles for Dual-Sensitive Release of Doxorubicin. *Macromol Rapid Commun.* **2018**, *29*, 20.

75. Yu, Q.; Xie, A.; Huang, F.; Li, S.; Xiao, Y.; Shen, Y. Photosensitive multifunctional poly(vinyl alcohol) micelles for enhanced antitumor effect. *Mater Sci Eng C Mater Biol Appl*. **2017**, *76*, 918-924.

76. Torchillin, V. P.; Tischenko, E. G.; Smirnov, V. V.; Chazoc, E. I. Immobilization of enzymes on slowly soluble carriers. *J. Biomed. Mater. Res*. **1977**, *11*, 223-235.

77. Heller, J., Helwing, R. F., Baker, R. W., and Tuttle, M. E. Controlled release of water-soluble macromolecules from bio erodible hydrogels. *Biomaterials*. **1983**, *4*, 22-23.

78. Chiellini, E.; Solare, R.; Leonard, G.; Giannasi, D.; Lisciani, R.; Mazzanti, G. New polymeric hydrogel formulations for the controlled release of interferon. *J. Controlled Release*. **1992**, *22*, 273-282.

79. Oyama, J.; Lera-Nonose, D.; Ramos-Milaré, ÁCFH. Potential of Pluronics® P-123 and F-127 as nanocarriers of anti-Leishmania chemotherapy. *Acta Trop*. **2019**, *192*, 11-21.

80. Palcsó, B.; Moldován, Z.; Süvegh, K.; Herczegh, A.; Zelkó, R. Chlorine dioxide-loaded poly(acrylic acid) gels for prolonged antimicrobial effect. *Mater Sci Eng C Mater Biol Appl*. **2019**, *98*, 782-788.

81. Hu, X.; Kim, C.J.; Albert, S.K.; Park, S.J. DNA-Grafted Poly(acrylic acid) for One-Step DNA Functionalization of Iron Oxide Nanoparticles. *Langmuir*. **2018**, *34*, 47, 14342-14346.

82. Janagam, D.R.; Wu L, Lowe TL. Nanoparticles for drug delivery to the anterior segment of the eye. *Adv Drug Deliv Rev*. **2017**, *122*, 31-64.

83. Ruiz-Gatón, L.; Espuelas, S.; Larrañeta, E.; Reviakine, I.; Yate, L.A.; Irache, J.M. Pegylated poly(anhydride) nanoparticles for oral delivery of docetaxel. *Eur J Pharm Sci*. **2018**, *118*, 165-175.

84. Cheng, J.; Tang, X.; Zhao, J.; Shi, T.; Zhao, P.; Lin, C. Multifunctional cationic polyurethanes designed for non-viral cancer gene therapy. *Acta Biomater*. **2016**, *30*, 155-167.

85. Heller, J. Ocular delivery using poly (ortho esters). *Adv Drug Deliv Rev*. **2005**, *57*, 14, 2053-2062.

86. Tagami T, Yoshimura N, Goto E, Noda T, Ozeki T. Fabrication of Muco-Adhesive Oral Films by the 3D Printing of Hydroxypropyl Methylcellulose-Based Catechin-Loaded Formulations. *Biol Pharm Bull*. **2019**, *42*, 11, 1898-1905.

87. Das, R.; Pal, S. Hydroxypropyl methyl cellulose grafted with polyacrylamide: application in controlled release of 5-amino salicylic acid. *Colloids Surf B Biointerfaces*. **2013**, *110*, 236-241.

88. Rao, S.; Tan, A.; Boyd, B.J.; Prestidge, C.A. Synergistic role of self-emulsifying lipids and nanostructured porous silica particles in optimizing the oral delivery of lovastatin. *Nanomed*. **2014**, *9*, 18, 2745-2759.

89. Yaghi, O.; O'Keeffe, M.; Ockwig, N. Reticular synthesis and the design of new materials. *Nature*.**2003**, *432***,** 705–714.

90. Gombotz, Y. R.; Pettit, D.K. Biodegradable Polymers for Protein and Peptide Drug Delivery. *Bioconjugate Chem.* **1985**, *6*, 332-351.

91. Makadia, H. K.; Siegel, S. J. Poly Lactic-co-Glycolic Acid (PLGA) as Biodegradable Controlled Drug Delivery Carrier. *Polymers*. **2011**, *3*, 1377-1397.

92. Pourali, M.; Peterson, A. M. Thermal Modeling of Material Extrusion Additive Manufacturing. *ACS Sympsium Series*. **2019**, *7*, 115-130.

93. Yang, L.; Chen, Y.; Wang, M.; Shi, S.; Jing, J. Fused Deposition Modeling 3D Printing of Novel Poly (vinyl alcohol) / Graphene Nanocomposite with Enhanced Mechanical and Electromagnetic Interference Shielding Properties. *Ind. Eng. Chem. Res.* **2020**, *59*, 16, 8066–8077.

94. Xu, C.; Quinn, B.; Lebel, L. L.; Therriult, D.; L'Espérance, G. Multi-Material Direct Ink Writing (DIW) for Complex 3D Metallic Structures with Removable Supports. *ACS Appl. Mater. Interfaces.* **2019**, *11*, 8, 8499-8506.

95. Spencer, A. R.; Sani, E.S.; Soucy, J.R.; Corbet, C. C.; Primbetova, A.; Koppes, R.A.; Annabi, N. Bioprinting of a Cell-Laden Conductive Hydrogel Composite. *ACS Applied Materials & Interfaces.* **2019**, *11*, 34, 30518-30533.

96. Weems, A.C.; Chiaie, K. R.; Yee, R.; Dove, A.P. Selective Reactivity of Myrcene for Vat Photopolymerization 3D Printing and Post Fabrication Surface Modification. *Biomacromolecules.* **2020**, *21*, 1, 163-170.

97. Herzberger, J.; Meenakshisundaram, V.; Williams, C.B.; Long, T. E. 3D Printing All-Aromatic Polyimides Using Stereolithographic 3D Printing of Polyamic Acid Salts. *ACS Macro Lett.* 2018, 7, 4, 493-497.

98. Li, X.; Yu, R.; He, Y.; Zhang, Y.; Yang, X.; Zhao, X.; Huang, W. Self-Healing Polyurethane Elastomers Based on a Disulfide Bond by Digital Light Processing 3D Printing. *ACS Macro Letters.* **2019**, *8*, 11, 1511-1516.

99. Li, R.; Yuan, S.; Zhang, H.; Zhu, W. 3D Printing of Mixed Matrix Films Based on Metal-Organic Frameworks and Thermoplastic Polyamide 12 by Selective Laser Sintering for Water Application. *ACS Appl. Mater. Interfaces*. **2019**, *11*, 43, 40564-40574.

100. Hao, Y.; Li, W.; Zhou, X.; Yang, F.; Qian, Z. Microneedles-Based Transdermal Drug Delivery Systems: A Review. *J. Biomed. Nanotech*. **2017**, *13*, 1581-1597.

CHAPTER 2

DRUG DELIVERY BY ZIF-8 AND PLGA COMPOSITE

2.1 Abstract

Delivery of drugs into the body for a prolonged period and keeping the drug molecules intact from different cellular environmental stresses- are two main challenges for the conventional drug delivery methods. In order to overcome these challenges, in this chapter, Zeolitic imidazole framework (ZIF)-8 has been combined with a biodegradable and biocompatible polymer poly (lactic-co-glycolic acid) (PLGA) to build a composite to deliver model drug Cy5, which is a far red fluorescent dye having excitation and emission maxima at 647 nm and 670 nm respectively, and can be easily detected. This composite is fabricated by loading Cy5 in ZIF-8 and preparation of PLGA microparticles with that Cy5-ZIF-8 particles by solvent evaporation method. An effort to deliver small Ultra Red Fluorescence Protein (smURFP) by this composite has also been discussed in this chapter.

2.2 Chemicals and Materials

2-methyl imidazole, zinc acetate dihydrate, sodium chloride, PBS buffer pH 7.4, poly lactic co glycolic acid (50:50; MW 30000-60000) and poly vinyl alcohol were purchased from Thermo Fisher Scientific (Waltham, MA, USA), Sigma Aldrich (St. Louis, MO, USA) and LACTEL (Birmingham, AL, USA). All the reagents were used without additional purification after receiving from the manufacturer. Cy5 dye was synthesized in Gassensmith Lab, UT Dallas.

2.3 Experimental

2.3.1 ZIF-8 preparation

ZIF-8 are metal organic frameworks composed of Zn ions and imidazole linkers. Different sizes

of ZIF-8 was prepared using previous protocol where 1085.7 mM 18.4 μL 2-methyl imidazole (HMIM) was reacted with 2518 mM 476.5 μL Zn Acetate and 505.1 μL milliQ water in 1ml Eppendorf tube.

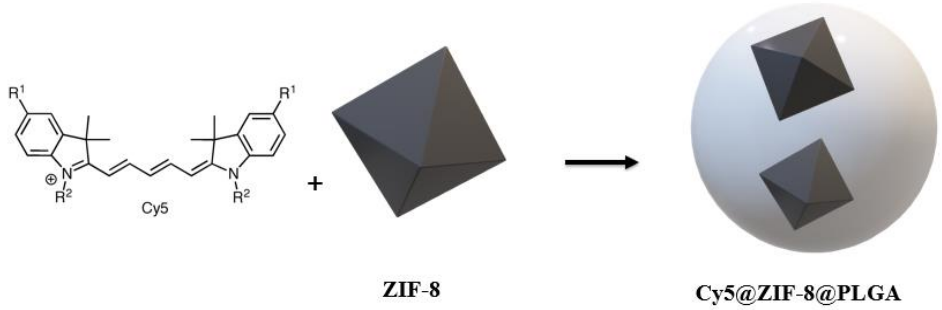

Figure 2.1 : Cy5 loading into ZIF-8 and final loading into PLGA

The ratio of Zinc acetate to HMIM concentration was kept 1:60. The reaction was done at room temperature for 24 h and washed with milliQ water twice and once with methanol and dried finally under air to get the ZIF-8 powders. This ZIF-8 is termed as 20×60 ZIF-8. A second batch of ZIF-8 was prepared by reacting 80 μL 1000 mM Zinc acetate and 640 μL 4000 mM 2-methyl imidazole (HMIM) and 280 μL milliQ water for 24 h at r.t. to keep the Zinc acetate to HMIM millimolar concentration at 80:32 ratio. This was washed twice with milliQ water and once with methanol. Further drying under air gave us white ZIF-8 powders which was termed as 80×32 ZIF-8. A third batch of ZIF-8 was prepared by reacting 1000 mM 40 μL Zinc acetate, 2000 mM 320 μL HMIM and 640 μL milliQ water for 24 h at r.t. to keep the Zinc acetate to HMIM millimolar ratio at 40:16. It was then washed and dried in the similar way to get the white crystalline ZIF-8 powders which was termed as 40×16 ZIF-8.

2.3.2 Synthesis of Cy5@ZIF-8

In order to load drug and easily track it, a model dye known as Cy5[1] was loaded inside 40×16 and 80×32 ZIF-8. This Cy5 dye was synthesized in Gassensmith Lab, Dept of Chemistry in UT Dallas. In Eppendorf tube 629 μL milliQ water was taken. Then 40 μL 1000 mM Zinc acetate and 10.9 μL 2.3 mg/ml Cy5 dye was added to that. The mixture was rotisseried for 15 minutes to mix them well. At last 320 μL 2000 mM HMIM was added to that and kept at room temperature in absence of air for 24 hours. After 24 hours they were centrifuged for 10 mins, 6000 rpm (3022×*g*) at Beckman micro centrifuge machine, washed with water twice and finally with methanol. After each wash the powder was centrifuged for 5 mins at 3022×*g*. Blue colored 40×16 Cy5@ZIF-8 powder was formed after drying in air.

In the similar way, 80×32 Cy5@ZIF-8 was prepared by adding 274 μL milliQ water, 80 μL 1000 mM Zinc acetate and 5.5 μL 1.8 mg/ml Cy5 dye in an 1 ml Eppendorf tube. This mixture was kept for 15 mins and then 640 μL HMIM was added and kept for 24 h reaction at room temperature. Then it was centrifuged at 9000 rpm (4533×*g*) in Beckman micro centrifuge machine for 15 mins. Then the precipitate was washed twice with milli Q water and once with methanol. After each wash centrifugation at 4533×*g* was done for 5 mins. Finally drying in air gave blue colored 80×32 Cy5@ZIF-8.

2.3.3 ZIF-8 PLGA microparticle preparation

A modified solvent evaporation method[2] was used to prepare the ZIF-8 microparticles. 0.05 g of 40×16 Cy5@ZIF 8 was taken and 0.1 g PEG-6000 was dissolved in Water to get 200mg /ml concentration. Then the ZIF was added to that by 20:1 w/w PEG:ZIF-8 ratio. The total volume was 5 ml. The solution was sonicated for 20 mins to dissolve ZIF-8. It was kept in freezer for

overnight at -80℃. The sample was collected from freezer and kept it for lyophilization. The sample was collected from the lyophilizer and washed with dichloromethane to remove extra the PEG-6000. It was taken in Eppendorf tubes and centrifuged for 3225×g for 10 mins and the precipitate was collected. This was done for 3 times. Then the sample was kept in vacuum evaporator for drying. Solid/Organic phase was prepared by suspending 20 mg of ZIF-8 microsphere powder in 2.5 ml DCM solution containing 125 mg PLGA.

PVA (2%) aqueous phase preparation:

5 gm PVA was taken and dissolved in enough water by boiling and stirring on a hot plate for 150 ˚C, 150 rpm for 2 h to get 250 ml solution. 1% NaCl (2.5 gm) was added to make 250 ml PVA aqueous solution. Then the oil phase was added to the 200 ml PVA solution and mixed with magnetic stirrer for 1.25 min at 340 rpm. Thus S/O/W emulsion was prepared.

Dilution: 1% NaCl containing 200 ml milli Q water was added and stirred with magnetic stir bar for 130 rpm for 12 hours. After 12 h PLGA particles were filtered by vacuum filtration and washing with water for three times and dried to get Cy5@ZIF-8 loaded PLGA particles.

80×32 Cy5@ZIF-8 was also used to prepare PLGA microparticles to see the change in their shapes and drug loading capacity. But the parameters needed to change compared to the 40x16 Cy5@ZIF-8 as aggregation was seen in case of 80×32 Cy5@ZIF-8 PLGA emulsion system.

2.3.4 Exfoliation of Cy5@ZIF-8 and Cy5@ZIF-8 loaded PLGA particles

In Eppendorf tube, 20 μg Cy5@ZIF-8 powder was mixed with 800 μl 0.5 M EDTA (pH 5.4) solution for 20 mins until the solution gets clear. Exfoliation of PLGA layer was done by adding 800 μL dicholomethane and butanol (1:1) solution to 10 μg PLGA particles in a 1 ml Eppendorf

tube. The Eppendorf tube was shaken for 10 mins and centrifuged to precipitate down the solid ZIF-8 particles.

Table 2.1 : Different reaction conditions of 80×32 Cy5@ZIF-8@PLGA microparticle preparation

Reaction conditions	**Batch prepared at 50ºC**	**Batch prepared at 60ºC**
Sample (Cy5@ZIF8) amount	70 mg	50 mg
Cy5@ZIF: PEG 6k	1:20	1:14
RPM of mixing	260	260
Mixing time (hrs)	18	18
Amount of PLGA	125 mg	125mg

2.3.5 Ex vitro study In order to observe the stability of PLGA microparticles in blood *ex-vitro* study was done by the presence of fluorescence intensity after treating the Cy5@ZIF-8@PLGA particles in 1×PBS buffer. The experiment was done at two different pH conditions. One was pH 7.4 which is the normal blood pH and another was pH 5.4 which mimic the extreme pH condition of blood in different disease state. The Fluorescence intensity was measured at different time intervals. For that four types of samples were prepared every time. In two Eppendorf tubes PBS buffer of pH 7.4 and 5.4 were taken and fluorescence intensity was measured and found no peaks. PLGA microparticles were dissolved in 1×PBS buffer pH 7.4 and pH 5.4 with 10 mins centrifugation in Beckman ultra-small centrifuge machine at 3225×*g*. Only the dissolved clear supernatant was taken and kept them in hot room (37 °C). In another two Eppendorf tubes Cy dye

was dissolved in 1×PBS buffer pH 7.4 and 5.4 and kept in the same condition as the PLGA microparticles to validate the change of fluorescence intensity of Cy5 dye at 37 ℃ .

2.4 Characterization

The sizes and shapes of all types of ZIF-8 powders and Cy5@ZIF-8 loaded PLGA particles were observed by Zeiss Supra 40 Scanning Electron Microscope (SEM) under high vacuum. The EHT of 2.4 KV and SE2 detector were used in all cases. Dynamic Light Scattering (DLS) was done by Malvern Zeta sizer machine to find the sizes of all the particles. UV and Horiba fluorescence machine were used to find out the concentration of Cy5 stock solution and the fluorescence intensity of the exfoliated particles in solution. Solid state fluorescence was also done to find out the presence of Cy5 in the ZIF-8 crystals. Powdered X-Ray Diffraction was done by Rigaku SmartLab XRD machine. The BET surface area of ZIF-8 was measured by porosity analyzer.

2.5 Result and Discussion

The one pot synthesis of ZIF-8 crystals showed different sizes with different molar concentration ratios of Zinc acetate and HMIM solutions in aqueous condition. The 1:60 ratio (20×60 ZIF-8) of these 2 solutions gave crystals having a size range of 389 nm to 795.5 nm. Likewise, 40×16 ZIF-8 (1:16 ratio) showed 1 μm to 1.3 μm size crystals where 1:32 ratio showed 80×32 ZIF-8 crystals of 264 nm to 304 nm. Biomineralization process led to the formation of 0.01 mg/ml Cy5 loaded ZIF-8 crystals. The Cy5 dye produced more nucleation sites in the reaction and thus the 40×16 crystal and 80×32 crystal's size was decreased a little bit compared to native 40×16 and 80×32 ZIF-8 crystals without Cy5.

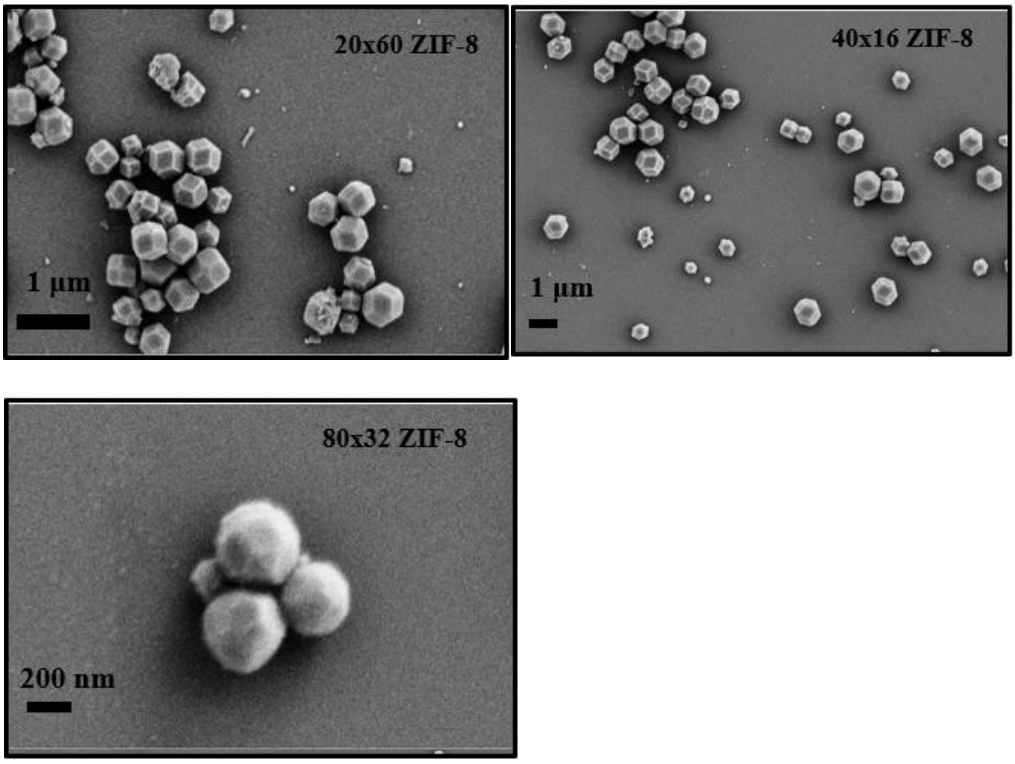

Figure 2.2 : SEM images of Crystal structure of 20×60 ZIF-8 (avg. size 500 nm), 40×16 ZIF-8 (avg size 1µm) and 80×32 ZIF-8 (avg. 300 nm)

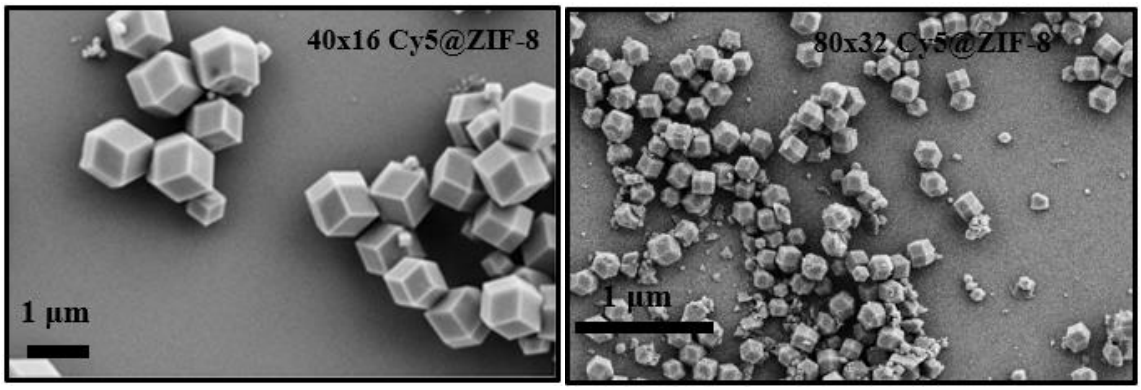

Figure 2.3 : SEM images of rhombic dodecahedron structures of Cy5 loaded 40×16 and 80×32 ZIF-8 crystals.

In the purpose of drug and vaccine delivery, ZIF-8 have shown promising application.[3-4] In order to reduce fast degradation in acidic condition, focus was given to prepare ZIF-8 polymeric nanoparticles to make it a powerful candidate. Here, the stability of ZIF-8 in blood and elimination

from body are important factors to take into consideration. Preparation of sustained release ZIF-8 can enable the release the ZIF-8 particles for many days and hence increase the stability of ZIF-8 in blood which leads to prolonged bioavailability of the drug molecules. To achieve that property, a biodegradable US FDA approved co-block polymer Poly-lactic-co-glycolic acid (PLGA) was used which consists of specific ratio of lactide and glycolide part and degrade by bulk erosion mechanism.[5] In this study 50:50 ratio of lactide and glycolide containing PLGA polymer has been used. The MW was 30,000-60,000 Dalton. Polymeric nano / microparticles are colloidal particles have sizes ranging from 1nm- 200 µm. They can be solid in oil in water (s/o/w) type emulsion or water in oil in water (w/o/w) type emulsion depending on type of the particle to be made polymeric. Inorganic particles have different procedure than the proteinaceous materials to encapsulate them inside the polymer matrix to make the emulsion. There are various known techniques to prepare the polymeric nano/ microparticles like double emulsion solvent evaporation[6], nanoprecipitation[7], supercritical fluid extraction[8] etc. For this work modified s/o/w solvent evaporation technique was used to prepare PLGA encapsulated ZIF-8 microspheres. The stability of the emulsion was also retained by maintaining osmotic pressure of the polymeric particles by 1% sodium chloride.

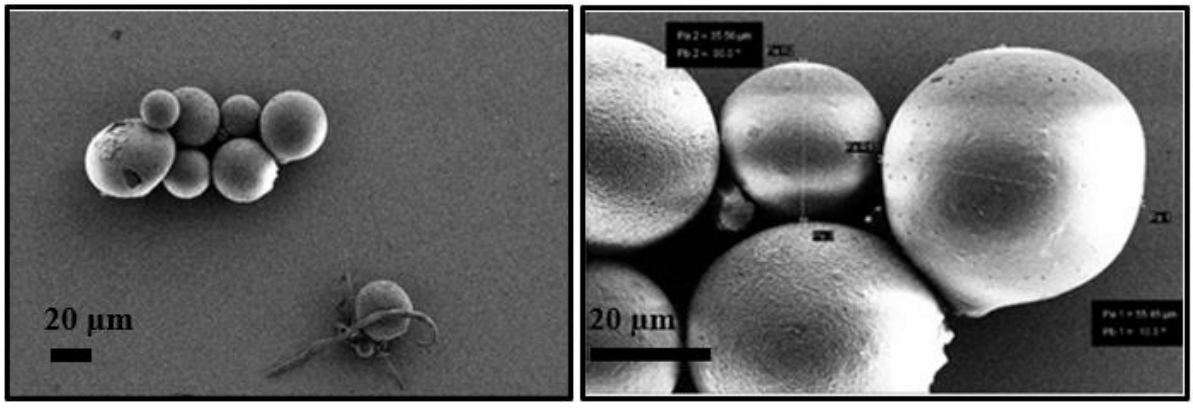

Figure 2.4 : SEM images of 40×16 Cy5@ZIF-8 loaded PLGA microspheres

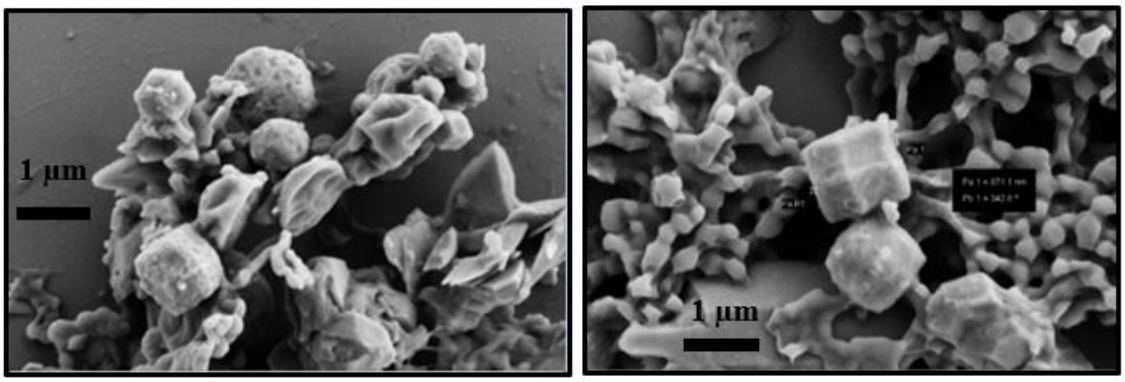

Figure 2.5 : SEM images after treatment of 40×16 Cy5@ZIF-8@ PLGA microspheres with chloroform- butanol (50 : 50) mixture. The images show the presence of ZIF-8 particles inside PLGA spheres

In order to prepare PLGA microspheres with 80×32 ZIF-8 different reaction temperatures were used: 25 ºC, 30 ºC, 50ºC and 60 ºC. But all other parameters were kept same. In case of 25 ºC and 30 ºC temperatures, the PLGA microspheres got aggregated. But at 50 and 60ºC temperatures, microspheres were seen (less than 100 µm diameter) without aggregation. Only microspheres prepared at 60 ºC had smooth surface which is needed for in vivo injection.

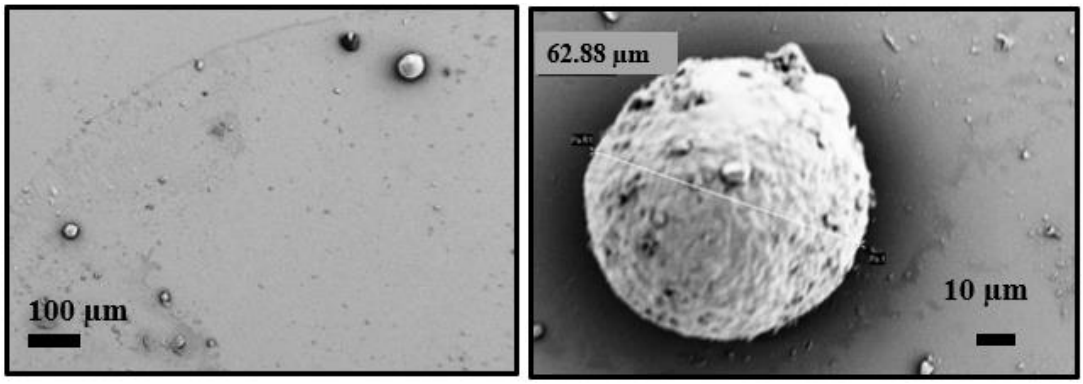

Figure 2.6 : SEM images of PLGA microspheres loaded with 80×32 Cy5@ZIF-8 (prepared at 60ºC)

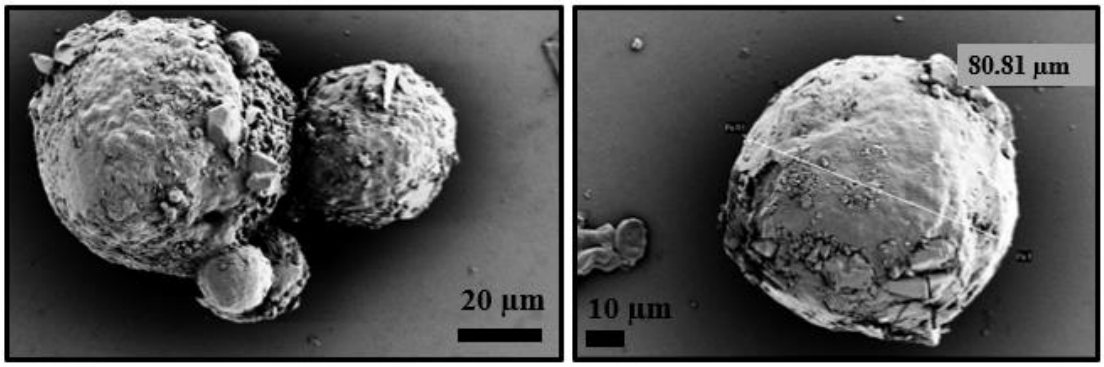

Figure 2.7 : SEM images of PLGA microspheres loaded with 80×32 Cy5@ZIF-8 (prepared at 50ºC)

Loading Efficiency In order to find the loading efficiency of Cy5 dye into the ZIF-8 Fluorescence study was done. The emission and excitation wavelength of the Cy5 dye is 647 nm and 670 nm respectively. A calibration curve was made with Cy5 fluorescence intensity vs concentration relationship. The fluorescence intensity was measured from the of the Cy5 dye stock solution first. Then after Cy5 loading and first centrifugation supernatant was collected from each Eppendorf tube and fluorescence intensity was again measured for that supernatant. From the difference of fluorescence intensity it was found that 40×16 ZIF-8 could load 90% Cy5 model drug and 80×32 ZIF-8 showed 92 % efficient loading of Cy5. In all cases the concentration of Cy5 stock solution was measured by UV Vis spectroscopic measurement by using beer lamberts law. The amount of Cy5 drug loaded in the PLGA microspheres were also measured. For this 1 mg of Cy5@ZIF-8 loaded PLGA particles were exfoliated by 1ml of 0.5 M (pH 5.4) EDTA solution for 2 hours. The fluorescence intensity of this exfoliated solution was measured and the concentration of the Cy5 dye was calculated from the calibration curve. It has been observed that each 1 mg of PLGA microparticles contain 0.23 mg of ZIF-8 and 6µg Cy5 dye.

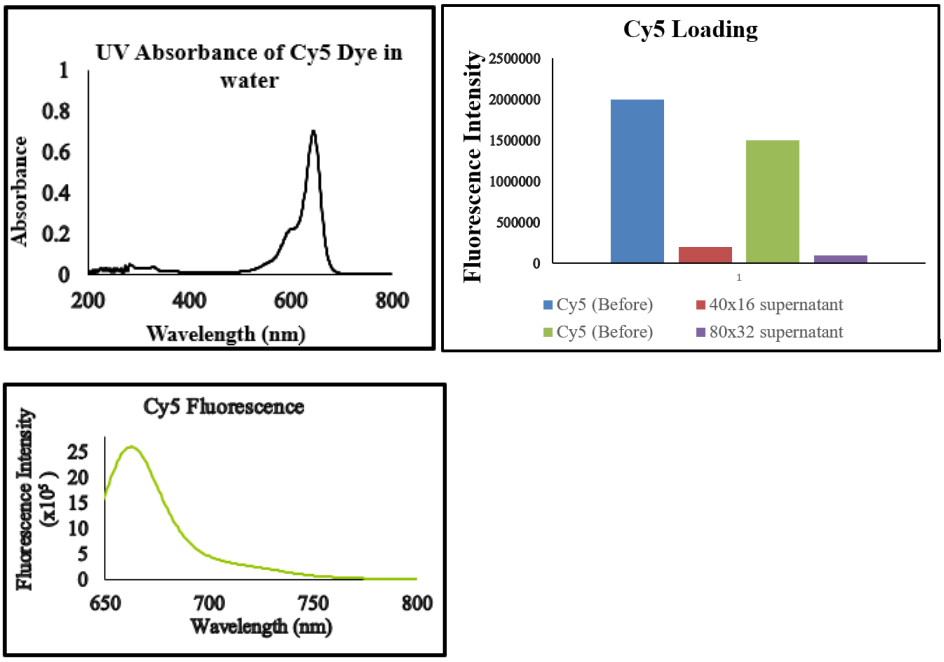

Figure 2.8 **:** UV-Vis and Fluorescence study on Cy5 dye (top left and bottom), Cy5 loading efficiency measurement by Fluorescence (top right).

The presence of Cy5 loaded ZIF-8 inside the PLGA microparticles was also confirmed by fluorescence study in water and methanol.

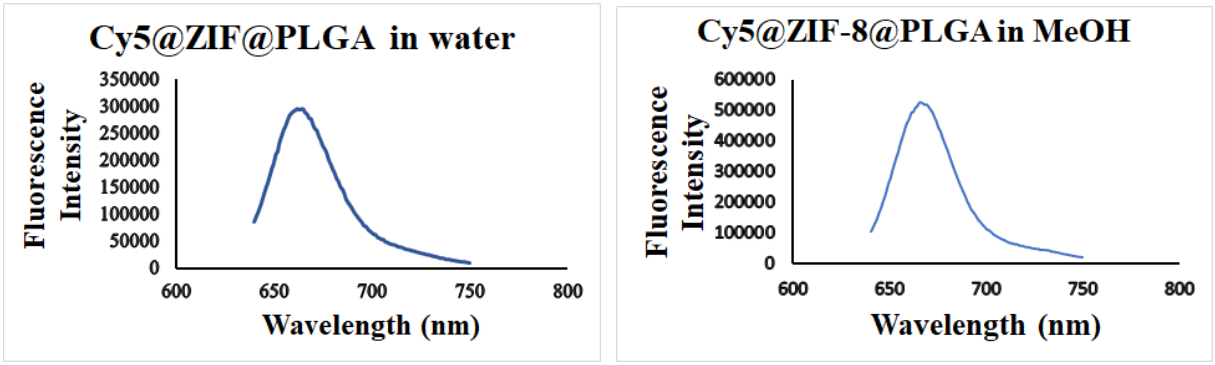

Figure 2.9 : Fluorescence study on Cy5@ZIF-8 loaded PLGA microspheres

Crystallinity To confirm the crystalline structure of ZIF-8 and Cy5@ZIF-8 powders PXRD was done and XRD patterns of 11.04°, 18.96°, and 23.92° 2θ confirmed the presence of ZIF-8

structures which was previously reported in literature.[9] As PLGA is a mixture of 50:50 crystal and amorphous character the irregular PXRD pattern confirmed the loading of Cy5@ZIF-8 in it.

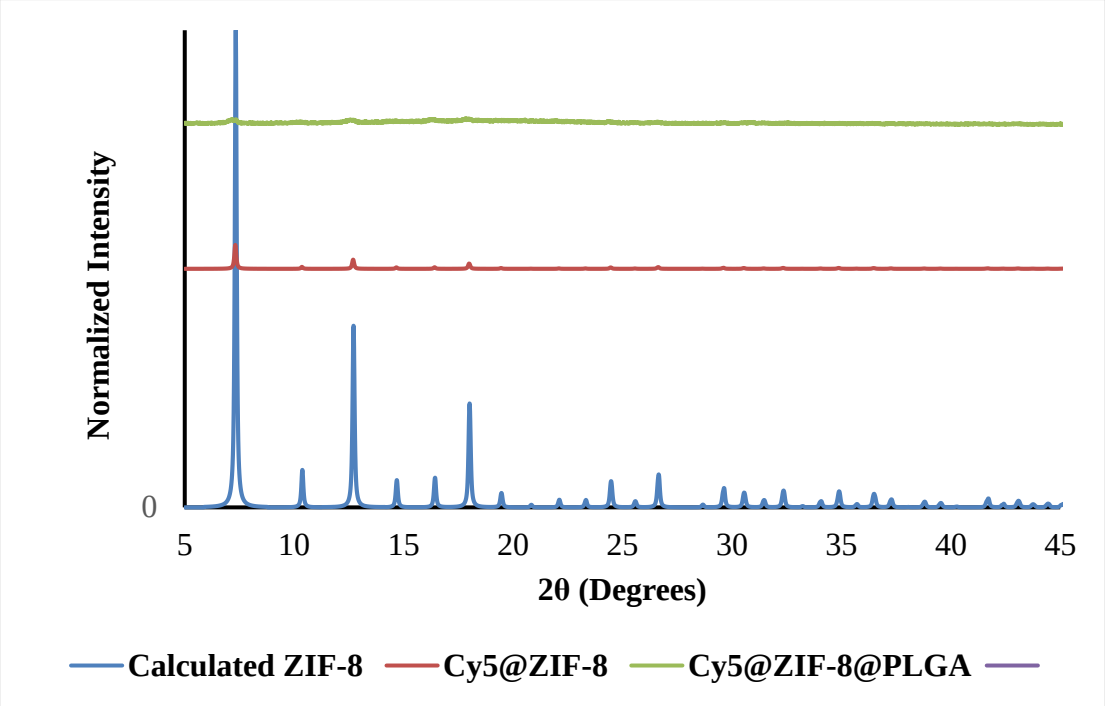

Figure 2.10 : Powdered XRD study on ZIF-8, Cy5@ZIF-8 and Cy5@ZIF-8 loaded PLGA microspheres.

DLS study

The sizes of Cy5@ZIF-8 particles and Cy5@ZIF-8 loaded PLGA microparticles were measured by Dynamic Light Scattering (DLS). This data complimented the sizes of particles found in SEM study. In case of 40×16 Cy5@ZIF-8 loaded PLGA particles the sizes of particles were ranged from 35 µm to 65.5 µm. Whereas, the sizes of 80×32 Cy5 loaded PLGA particles ranged from 21-67µm (60 ºC) and 20-81 µm (50 ºC) (Figure 2.11).

Ex Vitro Study on 40x16 Cy5@ZIF-8 loaded PLGA microparticles Incubation of Cy5 dye in 37 °C did not show any regular change of fluorescence intensity over time. Whereas, the PLGA

microparticles showed decrease in fluorescence intensity upto 6 days in both 7.4 and 5.4 pH conditions (Figure 2.12).

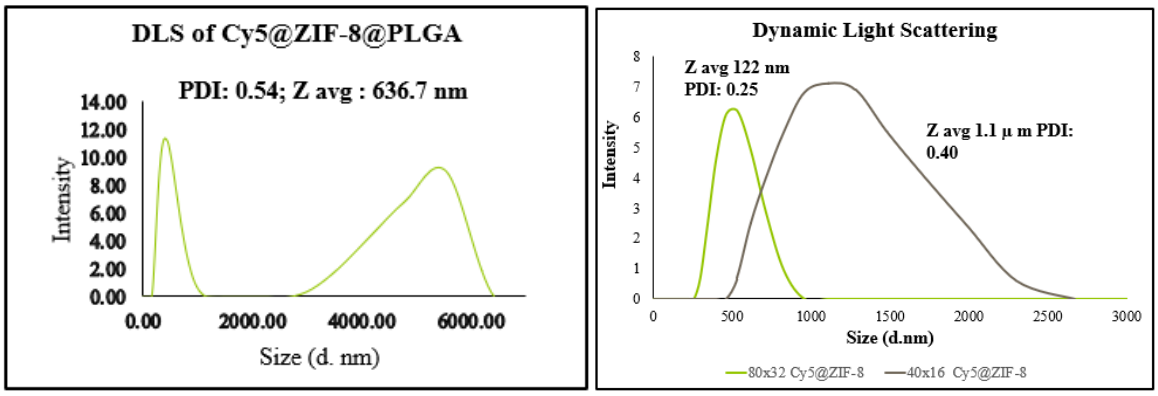

Figure 2.11 : DLS study on Cy5@ZIF-8 and Cy5@ZIF-8 loaded PLGA microspheres

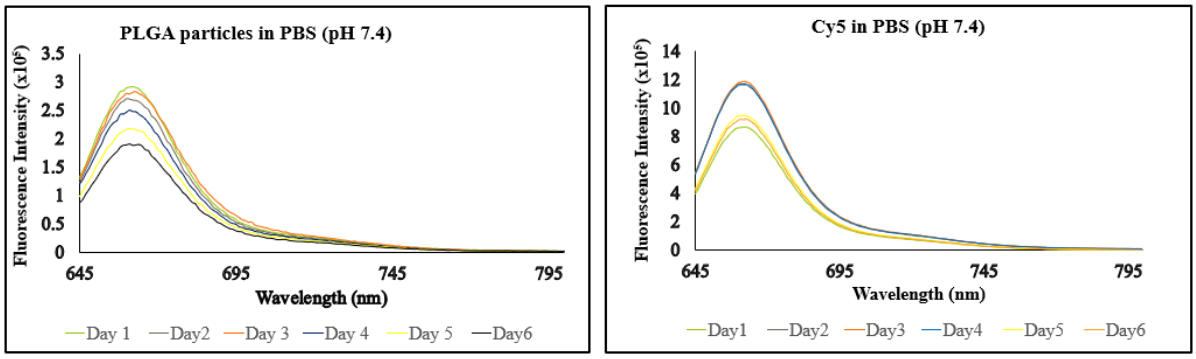

Figure 2.12 : Ex vitro study of 40×16 Cy5@ZIF-8 loaded PLGA particles

The *ex-vitro* experiment was done only for 6 days because further processing might quench the Cy5 dye which would give us false result. Hence, we can hypothesize that the PLGA microparticles are preserving the Cy5 dye in it and acting as sustained release protective shell which can enhance the release period of model drug Cy5 in blood pH.

***Ƶ* potential** Zeta potential of the particles were measured to see the change after PLGA encapsulation. As PLGA polymer created a shell around ZIF-8 *Ƶ* potential shown by Zn ions was lowered.

Table 2.2 : Ƶ potential study of Cy5@ZIF-8 loaded PLGA microparticles

Sample	Ƶ Potential (mV)
ZIF-8	+ 12.0
Cy5@ZIF-8	-3.13
Cy5@ZIF-8@PLGA	-5.103

2.6 Approach to deliver smURF Protein

Far red fluorescence proteins are desirable for *in vivo* imaging. Small ultra-red fluorescence protein (smURFP) is a class of far red fluorescent protein evolved from a cyanobacterial (*Trichodesmium erythraeum)* phycobiliprotein.[10] It is a homodimer with absorption and emission maximum of 642 nm and 670 nm and covalently attaches biliverdin (BV) without a lyase It has a large extinction coefficient (180,000 $M^{-1}cm^{-1}$) and quantum yield (18%), and comparable photostability to eGFP. SmURFP is extremely stable with a protein degradation half-life of 17 hour and 33 hour without and with chromophore (biliverdin), respectively. This is comparable to the jellyfish-derived enhanced green fluorescent protein (eGFP) protein degradation half-life of 24 hour.[11] SmURFP has significantly increased BV incorporation rate and protein stability compared to the bacteriophytochrome (BPH) FPs. In this study smURFP was expressed from *E.coli* from a heat shock method. It was then encapsulated in Zeolite imidazole network-8 (ZIF-8) as a proteinaceous model drug. To extend the release of proteinaceous drugs in blood this smURFP loaded ZIF-8 drug was encapsulated in a US FDA approved poly lactic co glycolic acid block polymer (PLGA) to prepare polymeric particles that can protect the ZIF-8 degradation in the blood which may prolong the release of smURFP in the blood.

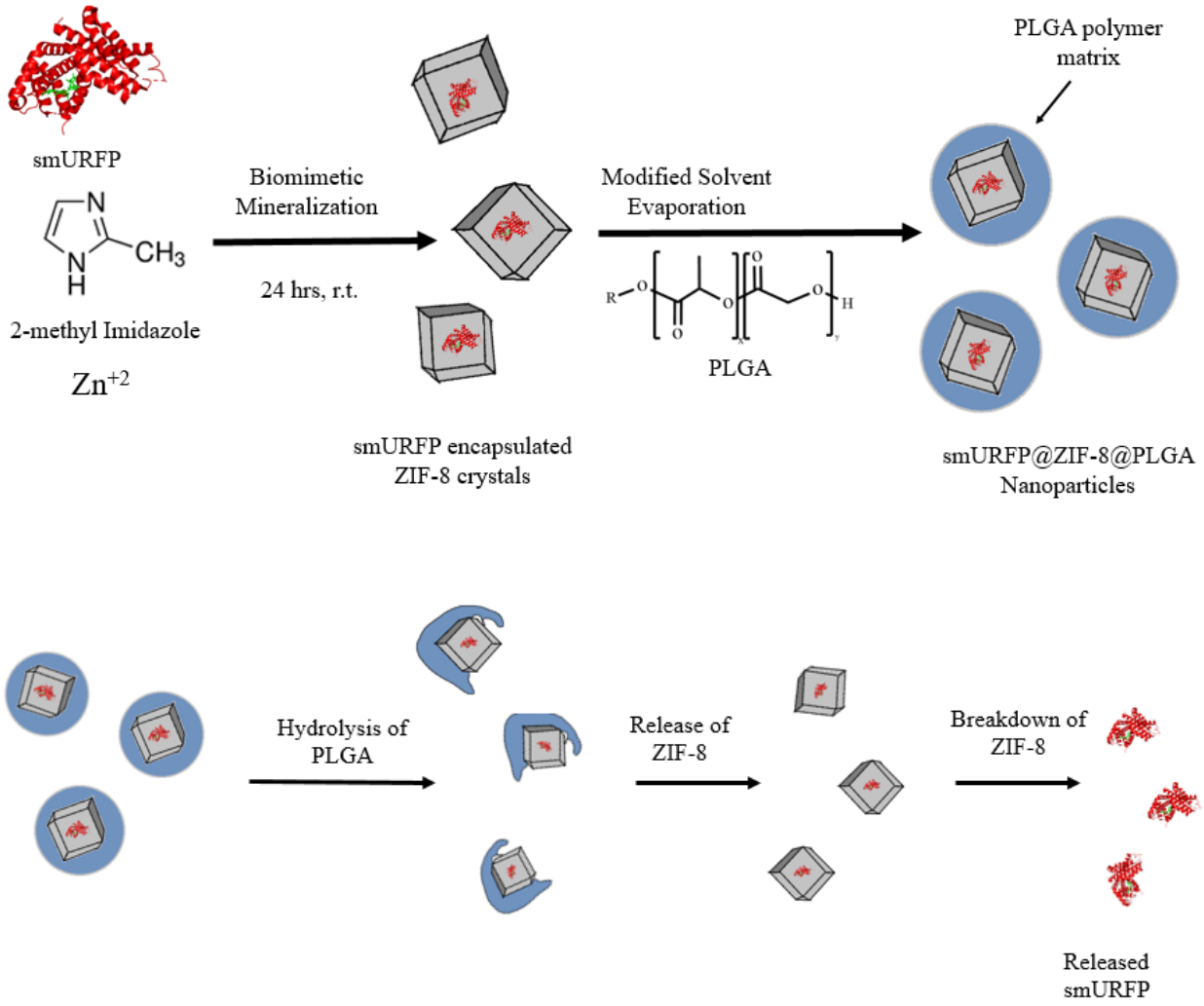

Fig 2.13 : Schematic diagram of smURFP delivery by ZIF8-PLGA system

2.6.1 Materials and Reagents

2-methyl imidazole, zinc acetate dihydrate, sodium chloride, PBS buffer pH 7.4, poly lactic co glycolic acid (50:50; MW 30000-60000) and poly vinyl alcohol were purchased from Thermo Fisher Scientific (Waltham, MA, USA), Sigma Aldrich (St. Louis, MO, USA) and LACTEL (Birmingham, AL, USA). All the reagents were used without additional purification after receiving

from the manufacturer. Cy5 dye was synthesized in Gassensmith Lab, UT Dallas. Small Ultra Red Fluorescent Protein was expressed and purified in Gassensmith Lab, UT Dallas.

2.6.2 Experimental and Result

Expression of smURFP

SmURF protein was expressed from E. coli by a heat shock method. On first day, yeast tryptone media was prepared. For each 1L media the recipe was:

Tryptone	20 g
Yeast extract	5 g
MgSO4	2.407 g
NaCl	0.5 g
KCl	0.186 g

The media was autoclaved at P20 or P30 cycle. 50ml / 100 ml of previously autoclaved media was transferred in a 125 ml /250 ml erlenmeyer flask respectively. One single *E. coli* bacterial colony was selected and added to 50 ml culture media and was shaken at 37 °C overnight. Starter culture was divided evenly between flasks and was shaken @ 37 °C until optical density reaches 0.8-0.9. To induce expression 10 g arabinose powder per liter was added and shaken overnight. Bacteria was palleted @ 10.5 K r.p.m. @ 4 °C for 10 mins and resuspended in pH 8 1×PBS buffer. Cells were lysated in microfluidizer. Cells were again palleted @ 10.5 K r.p.m. for 30 mins. FPLC was run with imidazole PBS solvent system to purify the smURF protein. Two characteristic peaks at 260 and 280 nm indicated the purified smURFP. It was then dialyzed for 72 h in a dialysis bag in old room (4 °C) to concentrate the smURFP. At last it was lyophilized to get pure intense blue colored smURF protein.

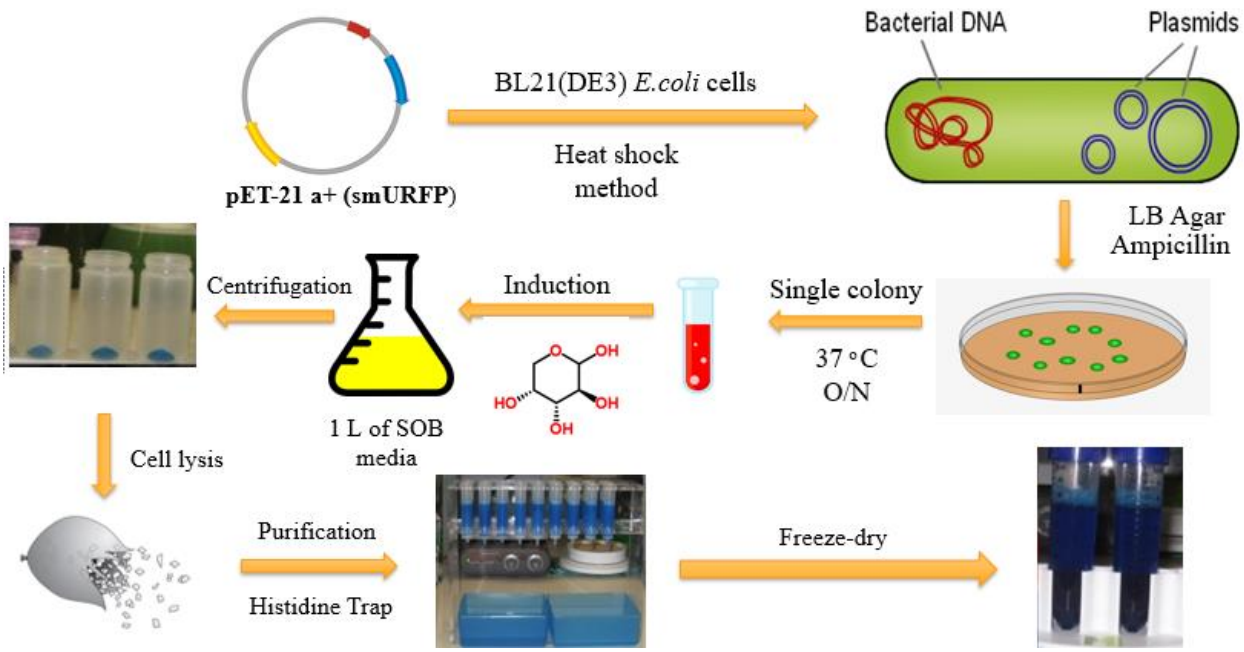

Figure 2.14 : Expression and purification of smURFP from *E. coli*

Preparation of smURFP@ZIF-8

Different concentrations of smURF protein (1 mg/ml, 0.2 mg/ml and 0.3 mg/ml) were tried to encapsulate into ZIF-8. 40: 640 ratio of Zn Acetate and 2-methyl imidazole reacted with different amounts of smURFP protein and milliQ water which resulted in smURFP encapsulated ZIF-8 powders.

Preparation of smURFP@ZIF-8@PLGA microparticles

A modified s/o/w method was used to prepare the ZIF-8 microparticles. 0.05 gm of smURFP@ ZIF 8 powder was taken. 0.1gm PEG-6000 was dissolved in Water to get 200mg /ml concentration. Then the ZIF was added to that by 1:20 w/w ZIF-8: PEG ratio. The total volume was 5 ml. The solution was sonicated for 20 mins to dissolve ZIF-8. It was kept in freezer for overnight at -80℃. The sample was collected from freezer and kept it for lyophilization. The sample was collected

from the lyophilizer and washed with dichloromethane to remove the PEG-6000. It was taken in Eppendorf tubes and centrifuged for 8000 rpm for 10 mins and the precipitate was collected. This was done for 3 times. Then the sample was kept in vacuum evaporator for drying. S/O phase was prepared by suspending 20 mg of ZIF-8 microsphere powder in 2.5 ml DCM solution containing 125 mg PLGA. 5gm PVA was taken and dissolved in enough water by boiling and stirring on a hot plate for 150 ˚C, 150 rpm for 2 h to get 250 ml solution. 1% NaCl (2.5 gm) was added to make 250 ml PVA aqueous solution. Then the oil phase was added to the 200 ml PVA solution and mixed with magnetic stirrer for 1.25 min at 340 rpm. Thus S/O/W emulsion was prepared. Then this mixture was stirred at room temperature at 230 rpm speed for 12 h to get the PLGA particles containing smURFP loaded ZIF-8 inside them. The particles were collected by three times washing with milli Q water.

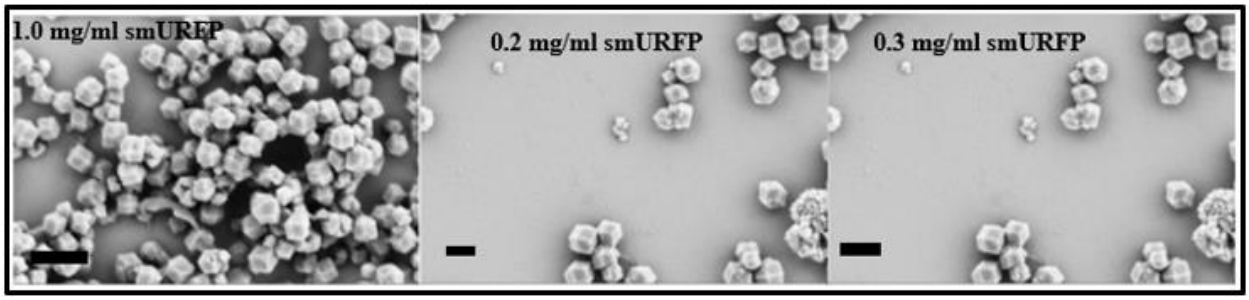

Figure 2.15 : Different concentrations of smURFP in ZIF-8 (Scale bar: 1µm)

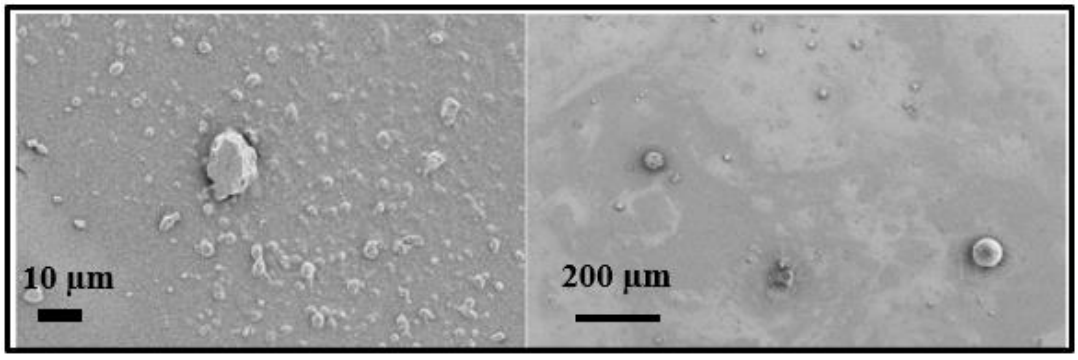

Figure 2.16 : smURFP@ZIF-8 PLGA particles

Fluorescence study: Solid and liquid state fluorescence data of smURFP@ZIF-8 and smURFP@ZIF@PLGA showed maximum emission at 670 nm after excitation at 642 nm which confirms presence of smURFP.

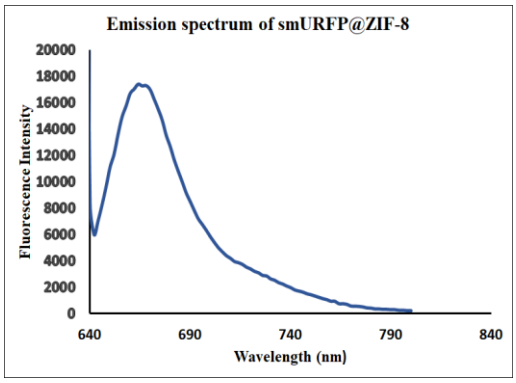

Figure 2.17 : Fluorescence study on smURFP@ZIF-8 particles

Gel Electrophoresis

smURFP@ZIF-8 particles was treated with exfoliation solution (0.5 M EDTA solution 600 µl, pH 7.9) and then ran through 1 % Agarose gel to see the presence of protein inside ZIF-8 molecules. After that it was imaged with Cy5 channel with Typhoon. The bright red bands indicated the presence of smURF proteins of different concentrations. The gel was also stained with Coomassie brilliant blue dye which also confirmed the protein inside the ZIF-8.

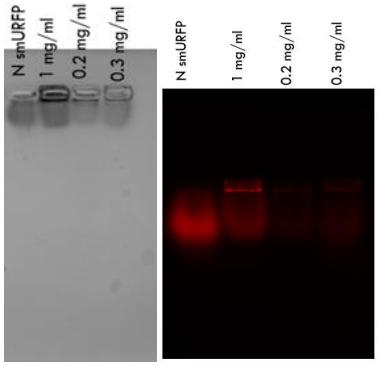

Figure 2.18 : 1% Agarose gel electrophoresis study on exfoliated smURFP@ZIF-8 crystals. smURFP@ZIF-8 after exfoliation. Typhon images of protein bands (right) and left image indicates protein bands after Comassie dye staining.

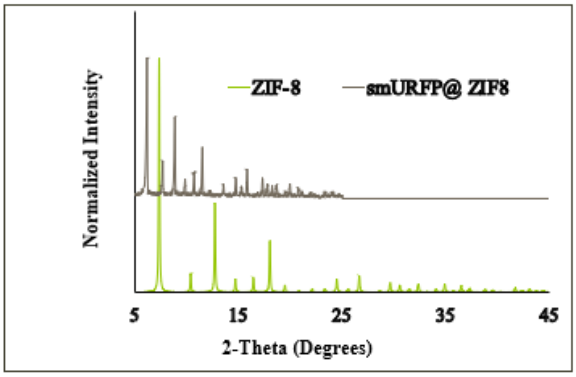

Figure 2.19 : PXRD of smURFP@ZIF-8

Powdered XRD data was taken with smart Rigaku XRD machine from 5 to 45 degrees. PXRD data clearly shows similarity of XRD pattern of ZIF-8 and smURFP@ZIF-8. That means encapsulation of smURFP did not change the structural integrity of ZIF-8.

2.7 Future Directions

Drug delivery by ZIF-8 and PLGA combination can be a strong delivery method to protect proteinaceous drugs from enzymes and unwanted degradation. Although it is a big concern whether the integrity of the protein molecules will be retained during the PLGA particle preparation. But we can be hopeful to retain the protein structure inside the ZIF-8 protective shell.

The optimum temperature for the preparation is a gap to find out. The *in vivo* study on mice model can also give us more insights and reveal the potential of this drug delivery tool.

2.8 References

1. Mujumdar, B; Ernst, A.; Mujumdar, SR.; Lewis, CJ.; Waggoner, AS. Cyanine dye labeling reagents: Sulfoindocyanine succinimidyl ester. *Bioconjugate Chemistry.* ***1993,*** *4, 105–11.*

2. Shi, W.; Didier, J. E.; Ingber, D. E.; Weitz, D. A. Collective Shape Actuation of Polymer Double Emulsion by Solvent Evaporation. *ACS Appl. Mater. Interface.* **2018**, *10*, 38, 31865-31869.

3. Li, S.; Dharmarwardana, M.; Welch, P.W.; Benjamin, C.; Shamir, A.M.; Nielsen, S. O.; Gassensmith, J.J. Investigation of Controlled Growth of Metal-Organic Frameworks on Anisotropic Virus Particles. *ACS Appl. Mater. Interfaces*. **2018**, *10*, 21, 18161-18169.

4. Zhang, Y.; Wang, J.; Ju, W. ; Liu, W.; Chen, Z.; Ren, J. Metal-Organic-Framework-Based Vaccine Platforms for Enhanced Systemic Immune and Memory Response. *Advanced functional materials*. **2016**, *26*, 6454-6461.

5. Gombotz, W. R.; Dean, K. P. Biodegradable Polymers for Protein and Peptide Drug Delivery. *Bioconjugate Chem*. **1995**, *6*, 332-351.

6. Teekampa, N. Polymeric microspheres for the sustained release of a protein-based drug carrier targeting the PDGFβ-receptor in the fibrotic kidney. *Int. J. of Pharmaceutics*. **2017**, *534*, 229-234.

7. Morales-Cruz, M. Two-step nanoprecipitation for the production of protein loaded PLGA nanosphere. *Results in Pharma Sciences.* **2012,** *2,*79–85.

8. Ahn, S.Y. Microfluidic spinning of fibrous alginate carrier having highly enhanced drug loading capability and delayed release profile. *RSC Adv.* ***2015,*** *5,* 15172-15181.

9. Adhikari, C.; Das, A.; Chakraborty, A. Zeolitic Imidazole Framework (ZIF) Nanospheres for Easy Encapsulation and Controlled Release of an Anticancer Drug Doxorubicin under Different External Stimuli: A Way toward Smart Drug Delivery System. *Mol. Pharmaceutics*. **2015**, *12*, 3158-3166.

10. Rodriguez, E. A.; Tran, G.N.; Gross, L. A.; Crisp, J. L.; Shu, X.; Lin, J. Y.; Tsien, R.Y. A far-red fluorescent protein evolved from a cyanobacterial phycobiliprotein. *Nat Method*. **2016**, *13(9),*763– 769.

11. Stack, J. H.; Whitney, M.; Rodems, S. M.; Pollok, B. A. A ubiquitin-based tagging system for controlled modulation of protein stability. *Nat. Biotechnology*. **2000**, *18 (12)*, 1298–1302.

12. Fuenzalida-Werner, J.P; Janowski, R; Mishra, K; Weidenfeld, I; Niessing, D; Ntziachristos, V; Stiel, A.C. Crystal structure of a biliverdin-bound phycobiliprotein: Interdependence of oligomerization and chromophorylation. *J. Structural Biology*. **2018,** *204 (3),* 519–522.

13. Chu, J.; Haynes, R. D; Corbel, S.Y.; Li, P.; González-González, E.; Burg, J. S; Ataie, N. J; Lam, A. J.; Cranfill, P. J. Non- invasive intravital imaging of cellular differentiation with a Bright red-excitable fluorescent protein. *Nat. Methods*. **2014**, *11 (5)*, 572–578.

14. Shaner, Nathan C.; Campbell, Robert E.; Steinbach, Paul A.; Giepmans, Ben N. G.; Palmer, Amy E.; Tsien, Roger Y. ,Improved monomeric red, orange and yellow fluorescent proteins derived from *Discosmosa* sp red fluorescence protein. *Nat. Biotechnology*. **2004**, *22* , 1567.

CHAPTER 3

DRUG DELIVERY BY ZIF-8 AND MICRONEEDLE COMPOSITE

3.1 Abstract

Additive manufacturing (AM) which is commonly known as 3-D printing is a process which can assemble highly customized complex structures from 3-dimensional data. In 3D printing we use different polymers to give them different geometric shapes. In this chapter we have used the Fused Filament Fabrication (FFF) 3D printing method to print poly lactic acid to fabricate biodegradable grids of sharp micron-sized protrusions capable of delivering therapeutic agents into the skin- known as microneedles which has gained focus in recent years as a minimally invasive and cost effective method for transdermal drug delivery. In order to enhance transdermal delivery of drug loaded ZIF-8 a biomineralization reaction has been introduced to prepare ZIF-8 coated microneedles.

3.2 Materials and Reagents

- Fluid Deposition Modelling Printer (Taz Lulzbot V5 and Mini 2 printer)
- Poly Lactic Acid (PLA) Filament
- Potassium Hydroxide
- Fusion 360 software

3.3 Experimental

3D modelling with Fusion 360

Fusion 360 software was used to do 3D modelling of different shapes of objects and microneedles of different sizes and lengths.

Printing Microneedles

Microneedles with different shapes and sizes were printed with Lulzbot Taz V5 and Lulzbot mini 2 printer. The Lulzbot Taz V5 has 0.3 mm nozzle head which was used for printing microneedles in our lab's previous microneedles paper.[1] In that paper our lab used etching method to produce microneedles with as low as 70 μm tip diameter. Previously our lab tried to print exactly cone shaped MNs. But the resolution of the printer did not permit to get that shape. So, we had to go for etching method to achieve that cone shaped MNs from cylinder shape MNs. So, our goal was to avoid etching step which was followed by further washing steps. In order to get rid of that, we thought to use Lulzbot mini 2 printer with 0.25 mm nozzle head and after optimizing many parameters in the printing condition we could achieve to get the perfect cone shaped MNs. We could also print some other shapes of MNs with poly lactic acid that we could not print before.

Loading ZIF-8 onto Microneedles

FITC Azide (0.01 mg/ml) loaded ZIF-8 was adsorbed onto the surface of the microneedle patches. For that water, 80 mM Zinc acetate, 0.01 mg/ml and 2560 mM HMIM solution was taken in a petri dish for reacting for 24 h. The microneedles patches were immerged into that solution. After 24 h the patches were removed and dried under vacuum.

3.4 Characterization

Zeiss Supra 40 Scanning Electron Microscopes was used to characterize the shapes and sizes of the printed microneedles. For that three minutes gold sputtering was done before taking SEM images. For imaging 2.4 kV EHT, SE2 gun and high vacuum condition was used. Differential Scanning Calorimetry (DSC) was done to find the melting and glass transition temperature of the

polymers used. Thermogravimetric analysis was done to see the polymer decomposition temperature.

3.5 Result and Discussion

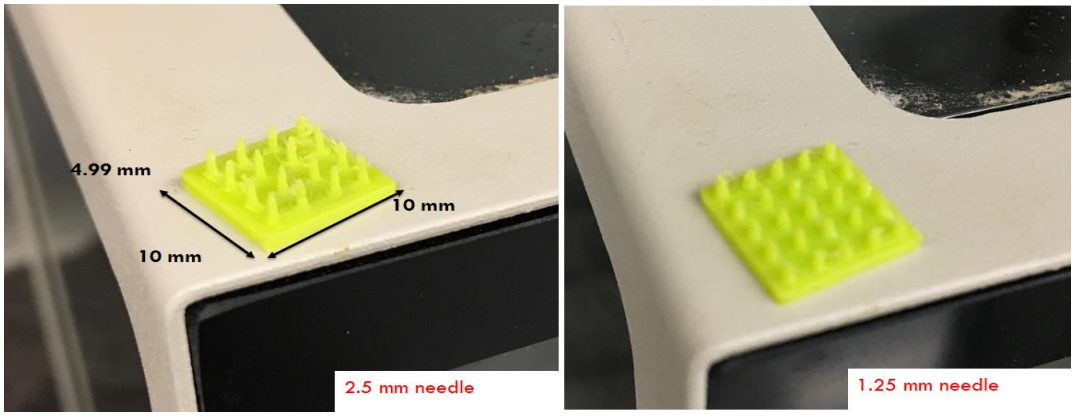

Figure 3.1 : Type 1 Microneedles printed by PLA

Type 1 MNs (both 4×4 and 5×5 arrays) were printed with printed 10 cm×10 cm sizes. The lengths of needles varied from 1.22 mm to 2.6 mm. The printing parameters that were used :Initial Layer Height: 0.1 mm, Printing temp: 205 ˚C, Bed temp:62 ˚C, Z offset: -1.68mm. The tip and base diameters for 2.5 mm needles were found to have 184 µm and 785 µm and for 1.25 mm it was found to have 167 µm and 1.075 µm. Although the tip size is greater than the previously etched MNs, this can be reduced by remodeling the STL files.

Type 4,5 & 6 MNs were also printed. Although these needles were not cone shaped they can be etched to give them pointy tip and different shapes of them may help to use them as breakable dissolving MNs.

Tests on Type 1 MNs Type 1 MNs were tested on 1.8 mm thick parafilm (equivalent to human skin mechanical strength) to ensure that these MNs can actually be inserted into human skin. 100% of the needles could go through the parafilm without breakdown.

Differential Scanning Calorimetry of Printing Material In order to show that the polymer characteristic of PLA was not changed after microneedles printing Differential Scanning Calorimetry (DSC) was done and no change in melting point before and after print was found. Although we could print cone shaped microneedles, but the tip size could not be reduced to 70 µm to be useful for insertion through skin. In order to do that the etching process could not be avoided. Different concentration of KOH was used for different period of time to optimize the etching process for already cone shaped needles.

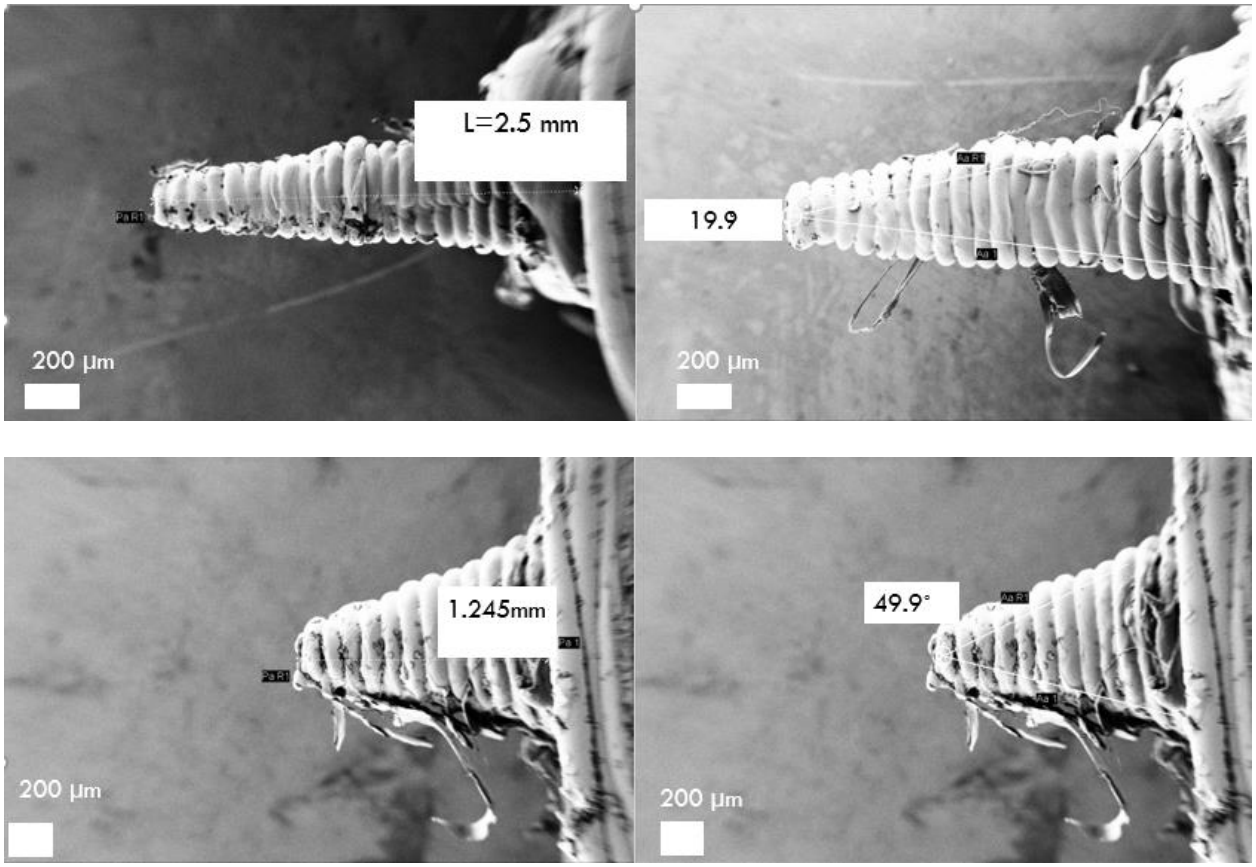

Figure 3.2 : SEM images of Type 1 Microneedles (2.5 mm length on the top and 1.25 mm at the bottom)

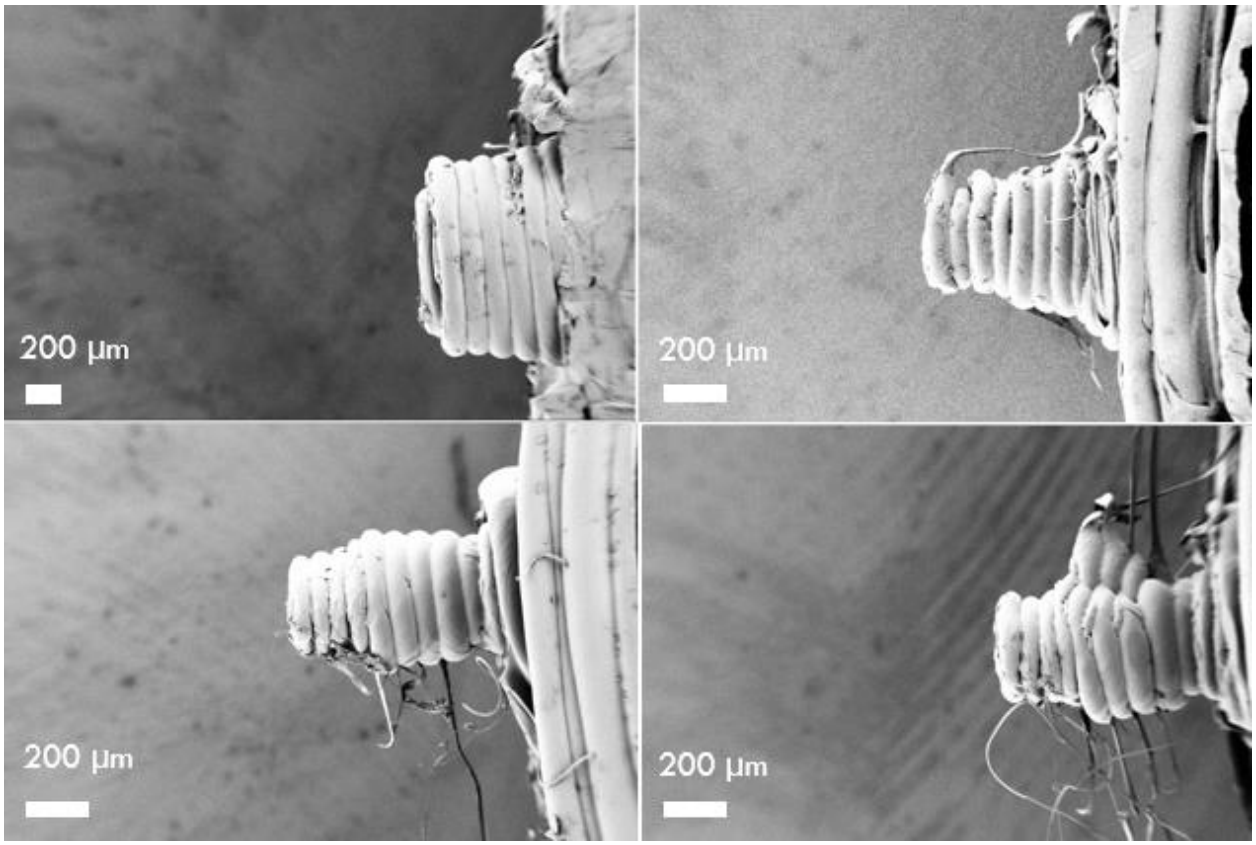

Figure 3.3 : SEM images of Type 4 (top left), Type 5 (Top right) and Type 6 (Bottom two) Microneedles.

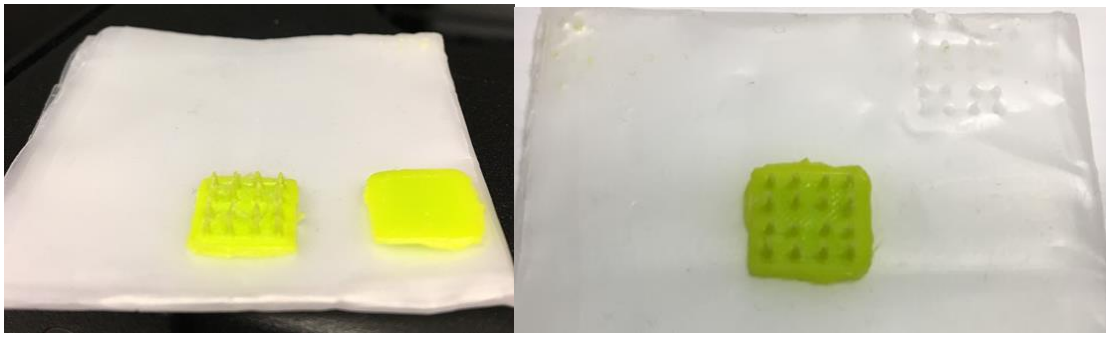

Figure 3.4 : Insertion test of Type 1 MNs into parafilm (1.8 mm).

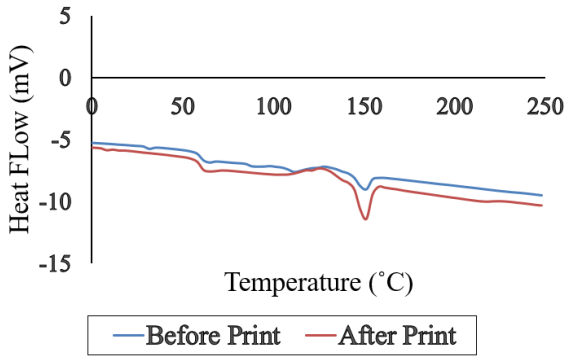

Figure 3.5 : Differential Scanning Calorimetry of PLA used in microneedles printing (before and after printing)

Table 3.1 : Etching of MNs for different time periods

3 hours	5 hours	6 hours	9 hours
No significant change	Small change in size	Change in size With mechanical strength upto 8.0 hrs	Changed a lot but brittle
Small change in size	Change in size	Change in size with mechanical strength upto 7.0 hrs	Changed a lot but brittle
Change in size	Change in size and mechanical strength intact	Change in size and mechanical strength Upto 6.5 hrs	Changed a lot but brittle

Etching and ZIF-8 Loading:

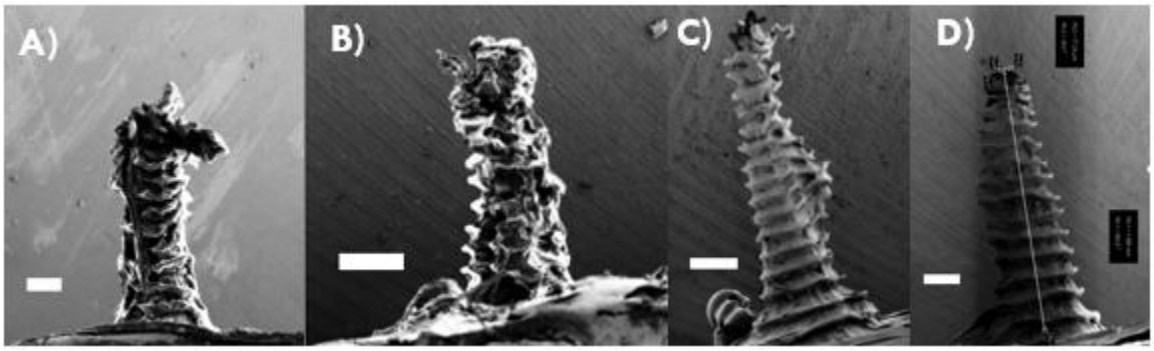

Figure 3.6 : Etched Microneedles with different concentration of KOH solution
A) 3M; 6.5 hr, B)5M; 6.5 hr, C)7M; 4.15 hr and D) 9M KOH; 4.15 hr etched MNs arrays

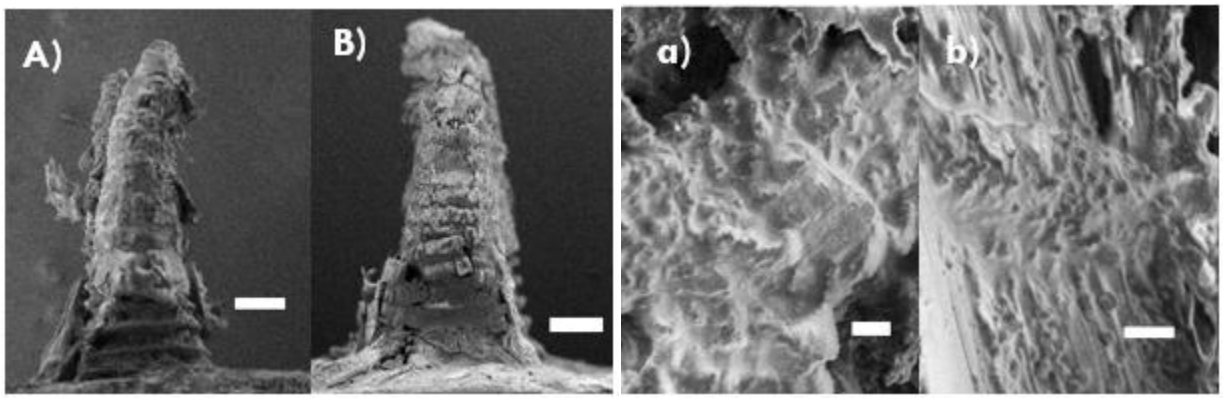

Figure 3.7 : 80×3 ZIF-8 Loaded MNs, A) 3 M KOH Ethced, B) 5M KOH Etched, (Scale bar: 200 µm) a) ZIF-8 growth in A) MNs, b) ZIF-8 growth in B) MNs by biomineralization, (Scale bar: 2 µm)

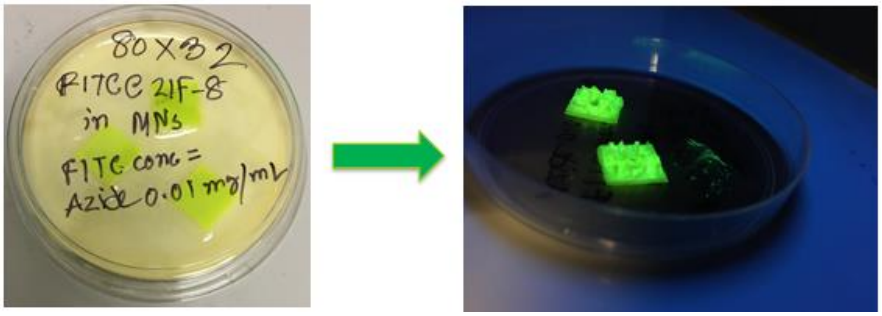

Figure 3.8 : Loading of FITC Azide and ZIF-8 in microneedles array

3.6 Polymer blending for making new materials for microneedles fabrication

Dissolving microneedles arrays are usually made of soft and biodegradable polymers that contain drugs and after insertion they get dissolved into skin and release drug molecules into the blood. In order to find a suitable material for that we selected polycaprolactone (PCL) which is a soft polymer having melting point of 60°C and a glass transition temperature of -60°C. Printing fine microneedles with PCL is not achievable due to it's softness and low mechanical strength. So, in order to achieve the mechanical strength, different percentages of polylactic acid (PLA) was blended with PCL by solvent casting method to make new material with sufficient mechanical strength and desirable softness. Thermogravimetric analysis was done to find the decomposition temperature of the PCL and PLA used and Differential Scanning Calorimetry was done for different blends of these two polymers. The melting temperature of PCL and PLA was changed and these data gave us an idea about the lower and upper limit of printing temperature.

Making Filament with blended polymer

A Filabot filament extruder was used to make filament with different blends of PCL and PLA. The diameter of the extruder nozzle was 3 mm and extrusion temperature was 170 °C. Although extruded filament was not of uniform diameter in all of it parts, this can be optimized by changing the temperature and collection method by using a spooler.

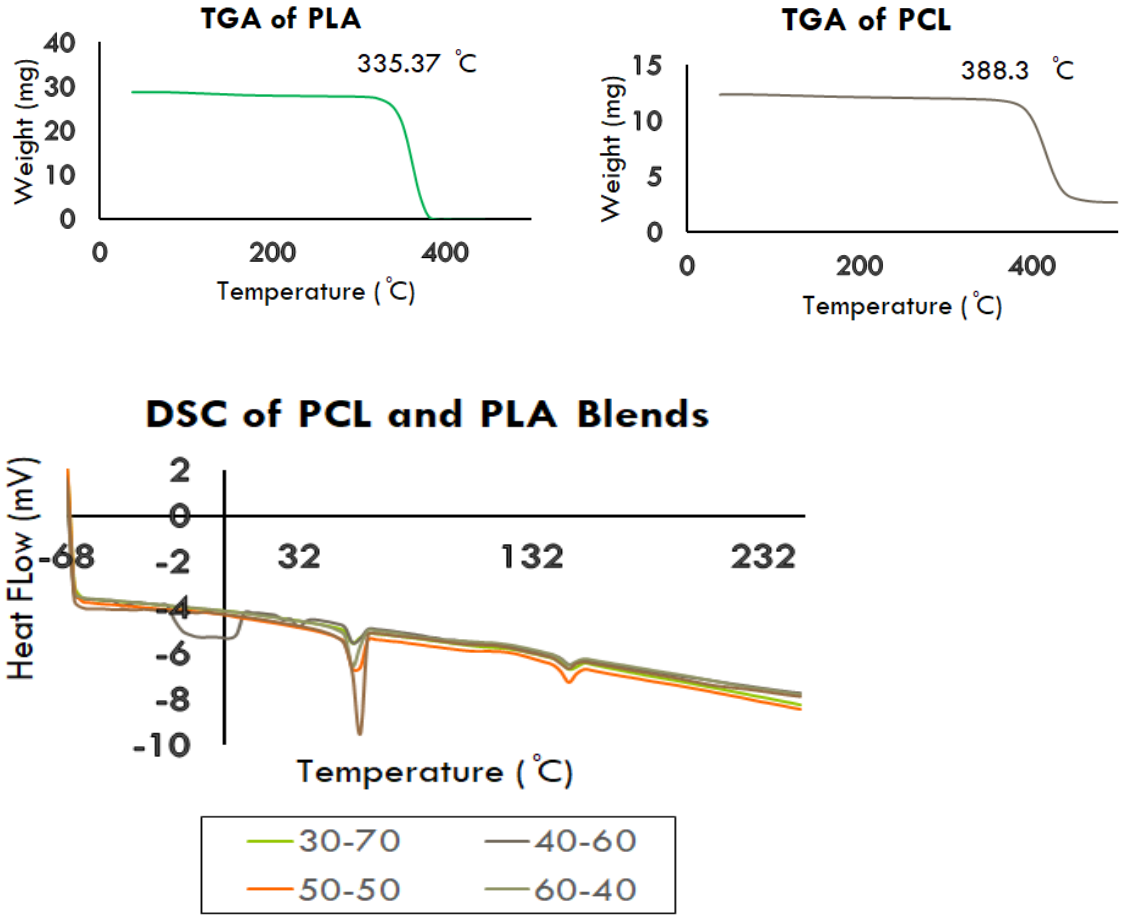

Figure 3.9 : Thermogravimetric analysis (TGA) curves of PLA and PCL and Differential Scanning Calorimetry graphs of different ratios of PCL/PLA blends.

Table 3.2 : Melting points of different PCL/PLA blends

PCL :PLA	Tm of PCL (℃)	Tm of PLA (℃)
30-70	51.54	148.07
40-60	51.54	148.07
50-50	54.85	148.07
60-40	54.85	148.07
70-30	58.19	148.07

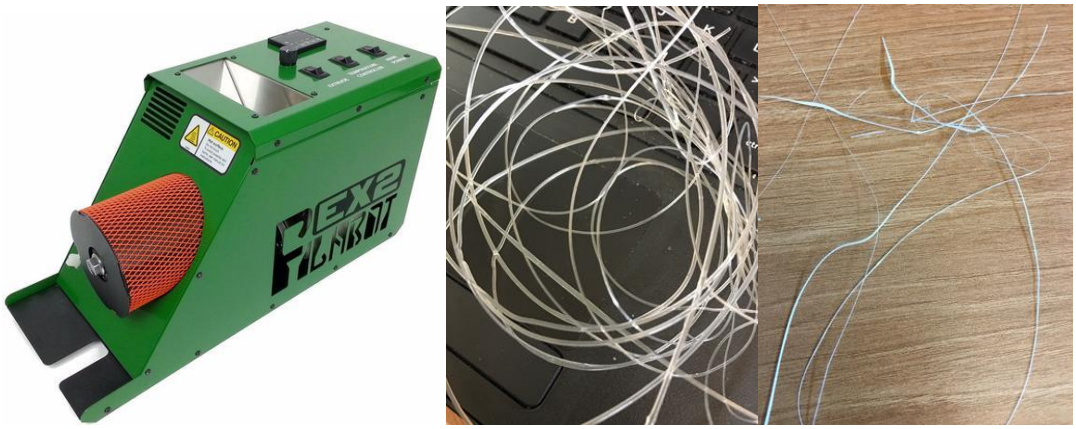

Figure 3.10 : (From left to right) Filament extruder, PCL filament, PCL:PLA=70:30 blended filament

3.7 References

1. Luzuriaga, M.A.; Berry, D.R.; Reagan, J.C.; Smaldone, R.A.; Gassensmith, J.J. Biodegradable 3D printed polymer microneedles for transdermal drug delivery. *Lab Chip*, **2018**, *18*, 1223-1230.

2. Zhu, M.; Liu, Y.; Jiang, F.; Cao, J.; Kundu, S.C.; Lu, S. Combine Silk Fibroin Microneedles for Insulin Delivery. *ACS Biomater. Sci. Eng.* **2020**, *6*, 6, 3422–3429.

3. Wang, S.; Zhu, M.; Zhao, L.; Kuang, D. Kundu, S.C.; Lu, S. Insulin Loaded Silk Fibroin Microneedles as Sustained Release System. *ACS Biomater. Sci. Eng.* **2019**, *5*, 4, 1887–1894.

4. Shim, D. H.; Nguyen, T.T.; Park, P.; Kim, M.; Park, J.; Lee, J.M. Development of Botulinum Toxin A-Coated Microneedles for Treating Palmar Hyperhidrosis. *Mol. Pharmaceutics.* **2019**, *16*, 12, 4913–4919.

BIOGRAPHICAL SKETCH

Tahmid Faisal was born in Dhaka, the capital city of Bangladesh. He completed his higher secondary school from Notre Dame College, Dhaka in 2009. In January 2010 he entered the University of Dhaka as an undergraduate student in the Department of Pharmacy. Tahmid received his Bachelor of Pharmacy degree in 2013 from the University of Dhaka. He received his Master of Pharmacy degree with a major in Pharmaceutical Chemistry in 2015 from the same university. His research area was phytochemistry. In the same year Tahmid started his professional career at Beximco Pharmaceuticals Ltd., Tongi, Bangladesh as a validation executive in Quality Assurance. In January 2016, Tahmid joined Stamford University Bangladesh as a lecturer in the Pharmacy department. In January 2017 he joined Southeast University, Bangladesh as a lecturer in the Pharmaceutical Science department and continued his service until July 2018. He moved to Dallas, TX, USA in August 2018 to attend the graduate program in Chemistry and Biochemistry at The University of Texas at Dallas.

CURRICULUM VITAE

TAHMID FAISAL

Graduate Teaching Assistant
Department of Chemistry and Biochemistry
The University of Texas at Dallas
800 West Campbell Rd., Richardson, TX, 75080
E-mail: tahmidfaisal3423@gmail.com linkedin.com/in/tahmid-faisal-5aa9538b
Tel: +1 (469)-879-5139

RESEARCH INTERESTS

- Pharmaceutics
- Drug Discovery and Design
- Polymer Chemistry
- Protein Chemistry

EDUCATION

- M.S. in Chemistry (Fall 2018-present), The University of Texas at Dallas, USA
  Current CGPA: 3.67

- M.Pharm., Department of Pharmaceutical Chemistry, University of Dhaka, 2015
  CGPA: 3.79 (Equivalent to 3.82 according to WES) on a scale of 4

- B.Pharm., Pharmaceutical Sciences, University of Dhaka, 2014
  CGPA: 3.70 (Equivalent to 3.89 according to WES) on a scale of 4

CURRENT RESEARCH

- Microneedles Drug Delivery by Fluid Deposition Model based 3D printing:
  This project covers the polymer filament development for biodegradable microneedles

  patches useful for transdermal drug delivery. (Fall 2018-present)

  Advisor: Prof. Dr. Ronald A. Smaldone, Dept. of Chemistry and Biochemistry,UT Dallas, TX. Reserach Lab :http://smaldonelab.com/

- Sustained release proteinaceous drug delivery by Zeolitic Imidazole Framework(ZIF-8) by combining polymer: Metal organic framework ZIF-8 is used for delivering protein, which has been combined with biodegradable polymer for prolonged in vivo therapy. (Fall 2018-present)
  Advisor: Prof. Dr. Jeremiah J. Gassensmith, Dept. of Chemistry and Biochemistry, UT Dallas, TX. Research Lab : http://labs.utdallas.edu/gassensmith/

PREVIOUS RESEARCH

- M.Pharm Thesis: Chemical and Biological investigations of Eurya acuminata (Theaceae)
  Advisor: Prof. Dr. A. T. M. Zafrul Azam, Dept. of Pharmaceutical Chemistry, University of Dhaka.

RESEARCH PUBLICATIONS

- Faisal, T.; Ahsan, M.; Choudhury, J. A.; Azam, A.T.M Z.; Phytochemical and Biological Investigations of Eurya acuminata (Theaceae). *Dhaka Univ.J. Pharm. Sci*. 2016, *15*, 2, 151-154.
- Zaman, S.; Islam, Md. S.; Koly, S. F.; Faisal, T.; Rakib, K. Evaluation of Cytotoxicity and Antibacterial Activities of Methanolic extract of Antidesma bunius (Linn.) (Family: Euphorbiaceae) Leaf. *J.Adv. Med. Pharm. Sciences*. 2018, 16, *2*, 1-7.
- Islam, Md S.; Faisal, T.; Munira, Mst S.; Ahammed, Md S.; Saha, S.; Afrin, S.; Ahammed, Md S. Islam, Md R. Poor Understanding of Prescribed Drugs Leads to Medication Error at Both Pharmacy and Patient End: A Survey Study to find Out the Underlying Factors. *Scientia Ricerca*. 2018, *2*, 4, 260-272.

SKILLS

- 3D Printing
- Scanning Electron Microscopy
- Softwares: Chemdraw, Autodesk Fusion 360

PROFESSIONAL EXPERIENCE

- Department of Chemistry and Biochemistry, UT Dallas,TX, USA
  - Teaching Assistant, (August 2018 - Present)
- Department of Pharmacy, Southeast University , Dhaka, Bangladesh
  - Lecturer, (January 2017 - July 2018)
- Department of Pharmacy, Stamford University Bangladesh, Dhaka, Bangladesh
  - Lecturer (January 2016 - January 2017)
- Beximco Pharmaceuticals Ltd., Dhaka, Bangladesh

- Validation Executive, Quality Assurance Department (July 2015 - January 2016)

AWARDS AND OTHER ACHIEVEMENTS

- Achieved National Science and Technology grand fellowship (NST) from the Govt. of peoples Republic of Bangladesh during M. Pharm , 2015
- Achieved Shahidullah Hall Merit Scholarship, University of Dhaka , 2015

GRADUATE COURSES

Advanced Organic Chemistry, Literature and Communication, Biophysical Chemistry,

Advanced Biochemistry, Advanced Analytical Chemistry

WORKSHOP AND SEMINARS

- Participated in The UT Dallas Chemistry Department Seminar Series (Fall 2018, Spring 2019, Fall 2019)
- Participated at workshop on *Quality Assurance in Higher Education* organized by Higher Education Quality Enhancement Project (HEQEP) in 2016
- Participated at*Good Manufacturing Process (GMP) training in Beximco Pharmaceuticals Ltd.* in 2015

CO-CURRICULAR ACTIVITIES AND COMMUNITY SERVICES

- Member of Chemistry Graduate Student Association, UT Dallas
- Member of Dhaka University Photographic society (DUPS)
- Member of Badhon a blood donation club of University of Dhaka
- Member of Dhaka University tourist society
- Member of Nature Study Society of Bangladesh.